Outage Performance of Dual-Hop UWB Transmissions Using a Multiple-Antenna Relay with Antenna Selection versus Single-Antenna Relay Selection

Kiattisak Maichalernnukul
Faculty of Information Technology, Rangsit University, Pathumthani, Thailand
Email: kiatti_m@hotmail.com

Abstract— **This paper presents one-way and two-way ultra-wideband (UWB) relay systems using a multiple-antenna relay with antenna selection and those using single-antenna relay selection. In particular, amplify-and-forward (AF) and detect-and-forward (DTF) relaying schemes are considered for these systems. The exact formulae for the end-to-end signal-to-noise ratio (SNR) outage probabilities of the one-way AF and one-way DTF relay systems are derived. In order to minimize these outage probabilities, the optimal power allocation strategies are presented. The SNR expressions for the received signals in the two-way AF and two-way DTF relay systems are derived to evaluate the system outage performance and to determine the corresponding optimal power allocation. Based on the above results, we quantify the effects of the number of antennas and the number of relays on the outage probabilities of the systems using the multiple-antenna relay with antenna selection and those using the single-antenna relay selection, respectively. We also compare such outage probabilities obtained with equal power allocation and the ones obtained with the aforementioned optimal power allocation strategies. Furthermore, the effect of spatial correlation at the multiple-antenna relay on the outage performance is studied. We find that in general, using the multiple-antenna relay with the antenna selection provides more outage gain than using the single-antenna relay selection for all the considered systems except the two-way DTF systems.**

Index Terms— **ultra-wideband (UWB), relay system, outage probability, antenna selection, relay selection**

I. INTRODUCTION

In the past few years, ultra-wideband (UWB) impulse radio (IR) has received significant attention due to its potential to deliver high data rates over short distances and to overlay spectrum with licensed narrowband radios [1], [2]. Because UWB-IR systems make use of extremely wide frequency bands where various legacy narrowband systems operate, their transmit power spectral density (PSD) is restricted according to the Federal Communications Commission (FCC) regulations [3], which leads to limited system coverage. One viable solution to this limitation is to employ relays as used in conventional cellular systems [4].

The potential for extending the coverage of the UWB-IR systems or improving their reliability through relaying has been demonstrated by many researchers [5]–[12]. While the work in [5]–[10] assumes that the relay(s) has (have) a single transmit/receive antenna[1], we investigated the benefits of multiple-antenna deployment at the relay(s) in [11], [12]. Such deployment is feasible if the space at the relays is available as in fixed relay networks, see, e.g., [13]. In [12], we also presented a performance comparison of a dual-hop relayed UWB transmission system using a single relay with multiple transmit/receive antennas (referred to as the multiple-antenna relay hereafter) and the one using multiple relays, each of which has one transmit/receive antenna (referred to as the single-antenna relay hereafter). This comparison showed that increasing the number of antennas at the multiple-antenna relay can generally yield a greater performance improvement than increasing the number of single-antenna relays. However, the gain obtained by deploying the multiple antennas comes at the price of hardware complexity. This is because the complexity and cost of the radio front end scale with the number of antennas [14], [15]. A possible way to reduce them while not sacrificing the gain too much is antenna selection. The first contribution in this paper is that we present the *exact* end-to-end signal-to-noise ratio (SNR) outage analysis of dual-hop UWB relay systems using a multiple-antenna relay with the antenna selection over a *UWB multipath fading channel*. Even though the main idea of this relaying scheme already exists in the *narrowband* relay systems (e.g., [16]), the unique properties of UWB-IR systems, such as *high multipath resolution* (which implies *a large number of resolvable paths*) and *carrierless transmission* [1], make the analyzed performance of the above UWB relay systems (where *only a subset of the resolvable paths can be practically utilized* owing to complexity constraints [17]) different from that of their narrowband counterparts. We also derive the optimal power allocation between the source and the relay to further enhance the system outage performance.

Recently, opportunistic relaying (also known as selection relaying), in which only the best relay(s) is (are)

Manuscript received March 3, 2012; accepted March 27, 2012.

[1]Throughout this paper, "transmit/receive antenna" means the antenna which can be used for reception as well as transmission.

doi:10.4304/jcm.7.4.329-348

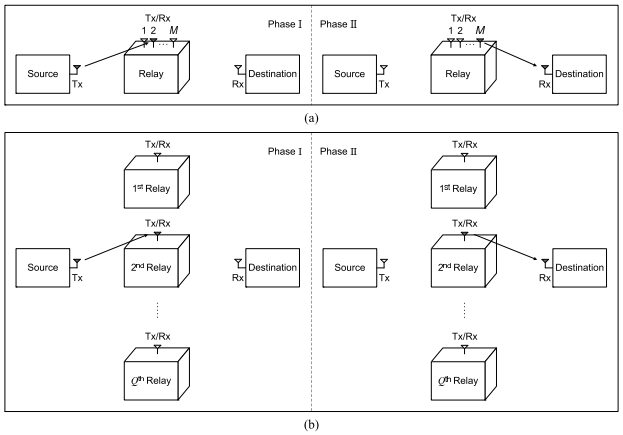

Figure 1. One-way half-duplex UWB relay system using: (a) a multiple-antenna relay with antenna selection; (b) the best relay among Q available single-antenna relays.

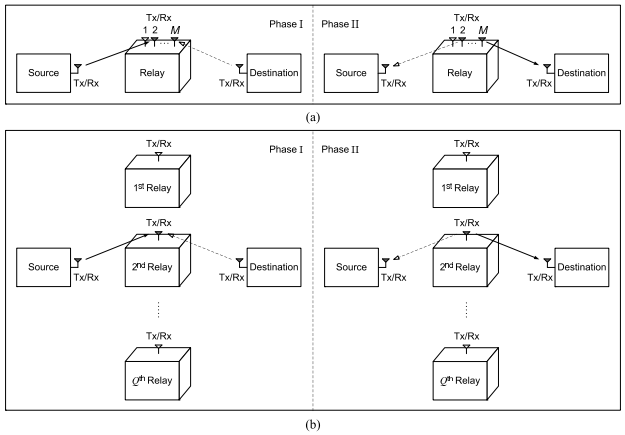

Figure 2. Two-way half-duplex UWB relay system using: (a) a multiple-antenna relay with antenna selection; (b) the best relay among Q available single-antenna relays.

chosen to be active among all available relays, has gained great interest since it suffers from no performance loss with less complexity compared to the deployment of all these relays [18]–[20]. In the literature, only a few papers have applied this simple technique to *multihop relayed UWB communications* [21]–[23]. In [21], [22], the opportunistic relaying was presented in the form of an efficient routing strategy for UWB ad hoc networks through cross-layer design. The work in [23] considered such relaying in UWB multiband orthogonal frequency division multiplexing (OFDM) systems. To the best of our knowledge, the performance of dual-hop UWB-IR systems with the relay selection has not been investigated yet in a UWB multipath environment. Hence, in this paper, we evaluate the performance of the systems in terms of end-to-end SNR outage probability, assuming that any of the available relays possesses one transmit/receive antenna. To minimize the system outage probabilities, the relay selection schemes combined with optimal power allocation are proposed. Note that the number of antennas used for per-hop data transmissions in these systems is the same as that in the systems using the multiple-antenna relay with the antenna selection (see the grey antennas in Figs. 1(a) and 1(b)). Both kinds of systems are of the same complexity roughly. We will compare their outage performance. In the comparison, *spatial correlation between the antennas* [24] at the multiple-antenna relay is taken into account.

Up to this point, we have considered only *one-way* half-duplex[2] communication scenarios. Most practical communications, however, are *two-way* in nature: the destination also has some data to send to the source. In order to improve the performance of source and destination transmissions *simultaneously*, we next extend the dual-hop UWB systems using the multiple-antenna relay with the antenna selection and those using the single-antenna relay selection to the case of *two-way relaying* (also known as bidirectional relaying) [26]–[29]. For clarity, the system model is shown in Fig. 2. In the first phase, both source and destination are scheduled to transmit simultaneously while the relay receives. In the second phase, the relay is scheduled to transmit while the source and destination receive. The main idea is that the source and destination, respectively, can cancel the *interference* (generated by their own transmissions) from the signals they receive from the relay, to recover the transmissions from the destination and source. Unlike prior work on two-way relaying which is mostly devoted to studying the relevant sum-rate performance in the narrowband context, this paper focuses on analyzing the *outage performance of those two-way UWB relay systems*. The power allocation strategies ameliorating the outage performance are introduced as well. It should be pointed out that our criteria for the antenna and relay selection in such systems similarly follow the criteria in the case of one-way relaying (see Sections III and IV), and thereby differ from the criteria considered in the previous work, see, e.g., [29].

The remainder of the paper is organized as follows: In Section II, the UWB channel model and the UWB relay system model are described. Sections III and IV present the relay systems using a multiple-antenna relay with antenna selection and those using single-antenna relay selection, respectively, both with their outage analysis and optimal power allocation. The extension of these systems to the case of two-way relaying is given in Section V. Section VI provides the numerical results, and Section VII concludes the paper.

Notation: $*$ denotes the convolution. $|\cdot|$ and $\mathtt{sign}(\cdot)$ denote the absolute value and sign operator, respectively. We use the notations $f_X(x;a,b)$ and $F_X(x;a,b)$ to refer to the probability density function (PDF) and cumulative density function (CDF) of the random variable X possibly

[2]Relaying transmissions can be classified into two main categories, namely *full-duplex* relaying and *half-duplex* relaying. The full-duplex relaying allows the relay to receive and transmit at the same time in the same frequency band, whereas reception and transmission for the half-duplex relaying are usually performed in time-orthogonal channels. Although the former relaying achieves higher spectral efficiency than the latter one, the large difference in power levels of the received and transmitted signals at the relay make it practically difficult to implement [25].

with parameters a and b, respectively. $\mathtt{E}[\cdot]$, $\mathrm{Var}[\cdot]$, and $\mathrm{Cov}[\cdot,\cdot]$ denote the expectation, variance, and covariance operators, respectively. The subscripts S, R, and D denote the source, relay, and destination in a relay system, respectively. $U(\cdot)$, $\Upsilon(\cdot,\cdot)$, $(\cdot,\cdot)$, and $\mathcal{K}_n(\cdot)$ denote the Heaviside step function, lower and upper incomplete Gamma functions, and n-th order modified Bessel function of the second kind defined in [30, eq. (17.13.93)], [30, eq. (8.350.1)], [30, eq. (8.350.2)], and [30, eq. (8.432)], respectively. $\binom{\cdot}{\cdot}$ is the binomial coefficient defined in [30, p. xliv].

II. Channel and System Models

In the literature on UWB channel models, there exist both *dense* and *sparse* multipath channels. In a dense multipath channel, observed for example in office and industrial environments [31], [32], each resolvable delay bin contains significant energy, and a tapped-delay-line (TDL) model with regularly-spaced arrival times of resolvable multipath components (as shown in (1)) gives a good approximation for the exact channel model. In some other environments, e.g., [33], [34], a sparse multipath channel has been observed, i.e., not every resolvable bin contains energy, and the arrival times are described as a continuous-time stochastic point process. The IEEE 802.15.3a/4a channel modeling subgroup proposed a modified Saleh-Valenzuela model as a reference channel model for such environments [35], [36]. In this model, the multipath arrivals were grouped into two different categories: a cluster arrival and a ray arrival within a cluster. Hence, it is much more complex than the aforementioned TDL model. In this paper, the theoretical analysis builds only on the TDL model (i.e., the case of dense channels) for analytical convenience. In Section VI, however, it will be shown that the performance trends in the cases of dense and sparse channels are similar.

Adopting the TDL model, we describe the channel impulse response (CIR) for a UWB transmission link as [31], [37]–[39].

$$h(t) = \sum_{l=0}^{L_t-1} \alpha_l \delta(t - lT_g) = \sqrt{G} \sum_{l=0}^{L_t-1} \varphi_l \delta(t - lT_g) \quad (1)$$

where L_t is the number of multipath components, l is the path index, α_l is the l-th path channel coefficient, T_g is the minimum multipath resolution, φ_l is the energy-normalized channel coefficient with $\mathrm{E}\left[\sum_{l=0}^{L_t-1}\varphi_l^2\right] = 1$, and G is the total multipath gain. The minimum multipath resolution T_g is equal to the width of the unit-energy monocycle pulse $g(t)$ used to convey data, as any two paths whose relative delay is less than the pulse width are not resolvable. The gain G is the reciprocal of the path loss, which is modeled as a function of the link distance and given in [31, eq. (1)]. We assume that $\{\varphi_l\}_{l=0}^{L_t-1}$ are mutually independent [39], and denote φ_l as $\varphi_l = \theta_l \upsilon_l$, where $\theta_l = \mathtt{sign}(\varphi_l)$ and $\upsilon_l = |\varphi_l|$. The variable θ_l takes the signs $+1$ and -1 with equal probability to account for the signal inversion due to reflection. The variable υ_l obeys the Nakagami-m distribution [31], [39] with the PDF given by

$$f_{\upsilon_l}(x; m, \eta_l) = \frac{2x^{2m-1}}{\eta_l^m (m-1)!} \exp\left(-\frac{x^2}{\eta_l}\right) U(x) \quad (2)$$

where $\eta_l = \Omega_l/m$, and $\Omega_l = \mathtt{E}[\upsilon_l^2]$ is exponentially decreasing with the excess delay, i.e., $\Omega_l = \varpi \Omega_{l-1}$ where $\varpi < 1$ is a constant. The value of ϖ is determined by the communication scenario. Throughout this paper, we assume that m is an integer and fixed for all the path indexes. The first assumption on m is necessary for the following theoretical analysis,[3] whereas the second one is just for analytical convenience. Define $\chi_l = \varphi_l^2 = \upsilon_l^2$. Hence, χ_l follows the Gamma distribution whose PDF and CDF, respectively, are

$$f_{\chi_l}(x; m, \eta_l) = \frac{x^{m-1}}{\eta_l^m (m-1)!} \exp\left(-\frac{x}{\eta_l}\right) U(x), \quad (3)$$

$$\begin{aligned} F_{\chi_l}(x; m, \eta_l) &= \left[1 - \frac{\left(m, \frac{x}{\eta_l}\right)}{(m-1)!}\right] U(x) \\ &= \left[1 - \exp\left(-\frac{x}{\eta_l}\right) \sum_{k=0}^{m-1} \frac{1}{k!} \left(\frac{x}{\eta_l}\right)^k\right] U(x). \end{aligned} \quad (4)$$

We consider two half-duplex dual-hop relayed UWB transmission systems: the one equipped with a relay possessing M transmit/receive antennas as shown in Fig. 1(a); and the one equipped with Q single-antenna relays as shown in Fig. 1(b). In both figures, the source and destination have one transmit antenna and one receive antenna, respectively. Throughout this paper, perfect timing and synchronization among the source, relay(s), and destination are assumed, and antipodal modulation signaling is used at the source and relay(s). Let $h_{\mathrm{S}q,j}(t)$ denote the CIR from the transmit antenna of the source to the j-th receive antenna of the q-th relay, and let $h_{q\mathrm{D},j}(t)$ denote the CIR from the j-th transmit antenna of the q-th relay to the receive antenna of the destination. Similar notations apply to the variables α_l, φ_l, and G contained in the corresponding CIR $h(t)$, as shown in (1). Then, we have that $\alpha_{\mathrm{S}q,j,l} = \sqrt{G_{\mathrm{S}q,j,l}}\varphi_{\mathrm{S}q,j,l}$ and $\alpha_{q\mathrm{D},j,l} = \sqrt{G_{q\mathrm{D},j,l}}\varphi_{q\mathrm{D},j,l}$. These channel coefficients are assumed to remain constant over the duration of the data transmission at both hops (i.e., the first and second phases in Fig. 1). Without causing confusion, we replace the index q with the subscript R and drop the index j in the relevant notations when considering them in Figs. 1(a) and 1(b), respectively. To make further analysis tractable, we assume that $\Omega_{\mathrm{S}q,j,l} = \Omega_{\mathrm{S}q,j',l}$ and $\Omega_{q\mathrm{D},j,l} = \Omega_{q\mathrm{D},j',l}$ for all l and $j \neq j'$. We ignore the direct link between the source and destination owing to the larger distance and additional path loss compared with the links between the

[3] This assumption may or may not be empirically true [40]. However, the channel modeled accordingly may still serve as a reasonable approximation to realistic UWB channels [39], [41]. Therefore, our outage analysis still provides insights into the performance of UWB relay systems.

source and relay and between the relay and destination.

III. Dual-Hop UWB Systems Using a Multiple-Antenna Relay with Antenna Selection

In these systems (see Fig. 1(a)), it is assumed that the relay has partial knowledge of the channels for the links from the source to the relay (denoted as S→R link) and from the relay to the destination (denoted as R→D link),[4] i.e., the relay knows the channel coefficients $\{\alpha_{\mathrm{SR},j,l}\}_{j=1,l=0}^{M,\,L-1}$ and $\{\alpha_{\mathrm{RD},j,l}\}_{j=1,l=0}^{M,\,L-1}$, where $L < L_t$. Let us denote $u = \arg\max_{j\in\{1,\ldots,M\}} \mathcal{E}_j$ where $\mathcal{E}_j = \sum_{l=0}^{L-1}\alpha_{\mathrm{SR},j,l}^2$, and denote $w = \arg\max_{j\in\{1,\ldots,M\}} \mathcal{E}'_j$ where $\mathcal{E}'_j = \sum_{l=0}^{L-1}\alpha_{\mathrm{RD},j,l}^2$. Notice that u may or may not be equal to w. Based on the above assumption, the relay selects only the u-th receive antenna to receive the transmitted signal from the source in the first phase. Likewise, in the second phase, only the w-th transmit antenna is selected by the relay to transmit a processed version of its received signal to the destination. In the following, we focus on two kinds of relaying schemes: amplify-and-forward (AF) relaying and detect-and-forward (DTF) relaying.[5]

A. Amplify-and-Forward Relaying

In the first phase, the source transmits the binary data bit b as [44]

$$x_{\mathrm{S}}(t) = b\sqrt{E_{f,\mathrm{S}}}\sum_{i=1}^{N_f} g(t-(i-1)T_f) \tag{5}$$

where N_f is the number of transmitted pulses that represent the data bit, T_f is the pulse repetition period, $E_{f,\mathrm{S}} = E_{b,\mathrm{S}}/N_f$ is the energy per pulse, and $E_{b,\mathrm{S}}$ is the energy of the data bit. Because the transmitted signal propagates through a UWB multipath channel described in (1), the pulse repetition period is chosen such that $T_f \geq L_t T_g$ to preclude intersymbol interference (ISI).[6] At the u-th receive antenna of the relay, a Rake receiver with L fingers, whose correlators use the pulse $g(t)$ as a template, is employed. The purpose is to achieve multipath diversity. Corresponding to the l-th finger, the correlator output can be written as

$$y_{\mathrm{R},u,l}(i) = b\sqrt{E_{f,\mathrm{S}}}\alpha_{\mathrm{SR},u,l} + n_{\mathrm{R},u,l}(i);\ l = 0,\ldots,L-1;\ i = 1,\ldots,N_f \tag{6}$$

where $n_{\mathrm{R},u,l}(i)$ is the additive white Gaussian noise (AWGN) with zero mean and double-sided PSD $N_0/2$. As the relay knows the channel coefficients $\{\alpha_{\mathrm{SR},u,l}\}_{l=0}^{L-1}$, the Rake combining output is given by

$$z_{\mathrm{R}} = \sum_{i=1}^{N_f}\sum_{l=0}^{L-1}\alpha_{\mathrm{SR},u,l}\, y_{\mathrm{R},u,l}(i). \tag{7}$$

Due to the availability of the channel coefficients $\{\alpha_{\mathrm{RD},w,l}\}_{l=0}^{L-1}$, a pre-Rake filter [46] with L taps (also called pre-Rake fingers) can be used at the w-th transmit antenna of the relay to exploit multipath diversity in the second phase. The transmitted signal from the relay is thus represented by

$$x_{\mathrm{R},w}(t) = \bar{z}_{\mathrm{R}}\sqrt{\frac{E_{f,\mathrm{R}}}{\mathcal{E}'_w}}\sum_{i=1}^{N_f}\sum_{l=0}^{L-1}\alpha_{\mathrm{RD},w,L-1-l}\, g(t-(i+N_f-1)T_f-lT_g) \tag{8}$$

where $\bar{z}_{\mathrm{R}} = z_{\mathrm{R}}/\sqrt{N_f\mathcal{E}_u(E_{b,\mathrm{S}}\mathcal{E}_u+N_0/2)}$, $E_{f,\mathrm{R}} = E_{b,\mathrm{R}}/N_f$ is the energy per pulse, and $E_{b,\mathrm{R}}$ is the energy of $\bar{z}_{\mathrm{R}}$. In the above equation, the Rake combining output z_{R} is normalized to be $\bar{z}_{\mathrm{R}}$ to ensure that the transmitted signal at the relay has the same average power as the one at the source if $E_{f,\mathrm{R}}$ is equal to $E_{f,\mathrm{S}}$. Note from (8) that the normalized output $\bar{z}_{\mathrm{R}}$ is modulated at the relay with the time-reversed version of the partial CIR for the R→D link. This results in a strong peak of the received signal at the destination and, therefore, only a matched filter (matched to the UWB pulse $g(t)$) is needed to receive this path [46], [47]. To gain a better understanding, let us first consider the received signal at the destination after passing through the matched filter and sampling, i.e.,

$$y_{\mathrm{D},l}(i) = \bar{z}_{\mathrm{R}}\sqrt{\frac{E_{f,\mathrm{R}}}{\mathcal{E}'_w}}\alpha_{\mathrm{RD},w,l} * \alpha_{\mathrm{RD},w,L-1-l} + n_{\mathrm{D},l}(i);\quad l = 0,\ldots,L-1;\ i = 1,\ldots,N_f \tag{9}$$

where $n_{\mathrm{D},l}(i)$ is the AWGN with the same statistical properties as $n_{\mathrm{R},u,l}(i)$. One can show that the term $\alpha_{\mathrm{RD},w,l} * \alpha_{\mathrm{RD},w,L-1-l}$ achieves its peak at $l = L-1$. As a result, the destination only needs

$$y_{\mathrm{D},L-1}(i) = \bar{z}_{\mathrm{R}}\sqrt{\frac{E_{f,\mathrm{R}}}{\mathcal{E}'_w}}\sum_{l=0}^{L-1}\alpha_{\mathrm{RD},w,l}^2 + n_{\mathrm{D},L-1}(i);\quad i = 1,\ldots,N_f \tag{10}$$

to form the decision variable for the data bit b, which is given by

$$z_{\mathrm{D}} = \sum_{i=1}^{N_f} y_{\mathrm{D},L-1}(i). \tag{11}$$

After some straightforward calculations, the overall end-to-end SNR, i.e., the SNR of z_{D}, is found to be

$$\gamma = \frac{\varrho_{\mathrm{S}}\,\mathcal{E}_u\ \varrho_{\mathrm{R}}\,\mathcal{E}'_w}{\varrho_{\mathrm{S}}\,\mathcal{E}_u + \varrho_{\mathrm{R}}\,\mathcal{E}'_w + 1} \tag{12}$$

where $\varrho_{\mathrm{S}} = \frac{E_{b,\mathrm{S}}}{N_0/2}$ and $\varrho_{\mathrm{R}} = \frac{E_{b,\mathrm{R}}}{N_0/2}$ are the transmitted SNRs at the source and relay, respectively. In Appendix

[4] The reason behind the *partial* CIR considerations is as follows. In typical UWB environments, the number of multipath components can be on the order of several tens [34]. From a practical point of view, only a subset of the multipath components can be exploited at the transmitter or receiver side [42].

[5] DTF is also referred to as *uncoded decode-and-forward* [43].

[6] For this non-ISI case, the AF scheme presented here is optimal. In the presence of ISI, which is beyond the scope of this paper, the presented AF scheme is suboptimal and some alternative relaying schemes, e.g., the filter-and-forward scheme in [45], would likely be preferable.

A, the CDFs and PDFs of $\mathcal{E}_u$ and $\mathcal{E}'_w$ are provided, and it is shown that for an arbitrary L, the closed-form expressions of these functions can be found only in *spatial uncorrelation case*. We focus on this case in the sequel, while the more general case, i.e., *spatial correlation case*, will be considered in Section VI.

Now, we derive the end-to-end SNR outage probability, which is used as the performance metric. This outage probability is given by

$$P_{\text{out}} = \Pr\left[\gamma \le \gamma_{\text{th}}\right] \tag{13}$$

where γ_{th} is a prespecified SNR threshold. By inserting (12) into (13), we get

$$\begin{aligned}
P_{\text{out}} &= \Pr\left[\frac{\varrho_{\text{S}}\,\mathcal{E}_u\;\varrho_{\text{R}}\,\mathcal{E}'_w}{\varrho_{\text{S}}\,\mathcal{E}_u + \varrho_{\text{R}}\,\mathcal{E}'_w + 1} \le \gamma_{\text{th}}\right] \\
&= \int_0^{\infty} \Pr\left[\frac{\varrho_{\text{S}}\,\varrho_{\text{R}}\,\mathcal{E}'_w\,x}{\varrho_{\text{S}}\,x + \varrho_{\text{R}}\,\mathcal{E}'_w + 1} \le \gamma_{\text{th}}\right] f_{\mathcal{E}_u}(x)\,dx \\
&= \int_0^{\frac{\gamma_{\text{th}}}{\varrho_{\text{S}}}} \Pr\left[\mathcal{E}'_w\,(\varrho_{\text{S}}\varrho_{\text{R}}\,x - \varrho_{\text{R}}\gamma_{\text{th}}) \le \gamma_{\text{th}}(\varrho_{\text{S}}\,x+1)\right] f_{\mathcal{E}_u}(x)\,dx \\
&\quad + \int_{\frac{\gamma_{\text{th}}}{\varrho_{\text{S}}}}^{\infty} \Pr\left[\mathcal{E}'_w\,(\varrho_{\text{S}}\varrho_{\text{R}}\,x - \varrho_{\text{R}}\gamma_{\text{th}}) \le \gamma_{\text{th}}(\varrho_{\text{S}}\,x+1)\right] f_{\mathcal{E}_u}(x)\,dx \\
&= \int_0^{\frac{\gamma_{\text{th}}}{\varrho_{\text{S}}}} f_{\mathcal{E}_u}(x)\,dx + \int_{\frac{\gamma_{\text{th}}}{\varrho_{\text{S}}}}^{\infty} F_{\mathcal{E}'_w}\!\left(\frac{\gamma_{\text{th}}(\varrho_{\text{S}}\,x+1)}{\varrho_{\text{S}}\varrho_{\text{R}}\,x - \varrho_{\text{R}}\gamma_{\text{th}}}\right) f_{\mathcal{E}_u}(x)\,dx \\
&= \mathcal{J}_1 + \mathcal{J}_2
\end{aligned} \tag{14}$$

where

$$\begin{aligned}
\mathcal{J}_1 &= F_{\mathcal{E}_u}\left(\gamma_{\text{th}}/\varrho_{\text{S}}\right) \\
&= 1 + \sum_{v=1}^{M} (-1)^v \binom{M}{v} \sum_{l_1=0}^{L-1} \sum_{k_1=1}^{m_{\text{SR}}} \cdots \sum_{l_v=0}^{L-1} \sum_{k_v=1}^{m_{\text{SR}}} \prod_{p=1}^{v} \Xi_{k_p} \left(\frac{\gamma_{\text{th}}}{\varrho_{\text{S}}}\right)^{A_1} e^{-\frac{A_2\gamma_{\text{th}}}{\varrho_{\text{S}}}},
\end{aligned} \tag{15}$$

$\mathcal{J}_2$ is shown at the top of the next page, Ξ_{k_p}, $\Xi'_{k'_{p'}}$, $\{A_n\}_{n=1}^{4}$, and $\Delta(l, k, m_{\text{SR}}, \{\Phi_{\text{SR},\ell}\}_{\ell=0}^{L-1})$ are defined in Appendix A. The detailed derivation of $\mathcal{J}_2$ is given in Appendix B.

To get an insight into the effect of some parameters (e.g., the number of antennas M) on the system performance from (14), we consider the following special case:

For $L = 1$, $m_{\text{SR}} = m_{\text{RD}} = 1$, $\varrho_{\text{S}} = \varrho_{\text{R}} = \varrho$, $\Phi_{\text{SR},0} = \Phi_{\text{RD},0} = \Phi$, and $\varrho\Phi >> 2M\gamma_{\text{th}}$, (14) simplifies to

$$\begin{aligned}
P_{\text{out}} \approx &\left[1 - \exp\left(-\frac{\gamma_{\text{th}}}{\varrho\Phi}\right)\right]^M \\
&\times \left[1 + M \sum_{v=0}^{M-1} \frac{(-1)^v}{v+1} \binom{M-1}{v} \exp\left(-\frac{(v+1)\gamma_{\text{th}}}{\varrho\Phi}\right)\right]
\end{aligned} \tag{17}$$

where we have used [48, eq. (9.6.9)] and [30, eq. (1.111)]. It is obvious from (17) that increasing the number of antennas decreases the outage probability. In more general cases, the benefit of multiple-antenna deployment will be demonstrated by numerical examples in Section VI.

B. Detect-and-Forward Relaying

In the first phase, the transmitted signal at the source and the received signal at the relay are the same as (5) and (6), respectively. The relay performs the data detection by producing the estimate of the transmitted bit as (7) and making a hard decision on it. The detected bit is given by $\hat{b}_{\text{R}} = \texttt{sign}(z_{\text{R}})$. This hard decision results in superior performance compared to the AF relaying scheme, as will be seen in Section VI. For the second phase, the transmitted signal at the relay and the received signal at the destination can be expressed, respectively, as (8) and (10) with $\bar{z}_{\text{R}}$ being replaced by $\hat{b}_{\text{R}}$. Finally, the decision variable can be obtained as (11). It is straightforward to show that the received SNRs for the S→R link and R→D link are, respectively,

$$\gamma_{\text{SR}} = \mathcal{E}_u\,\varrho_{\text{S}}, \tag{18a}$$

$$\gamma_{\text{RD}} = \mathcal{E}'_w\,\varrho_{\text{R}}. \tag{18b}$$

Accordingly, the end-to-end SNR outage probability can be derived as follows:

$$\begin{aligned}
P_{\text{out}} &= \Pr\left[\texttt{min}(\gamma_{\text{SR}}, \gamma_{\text{RD}}) \le \gamma_{\text{th}}\right] \\
&= 1 - \Pr\left[\gamma_{\text{SR}} > \gamma_{\text{th}}\right] \Pr\left[\gamma_{\text{RD}} > \gamma_{\text{th}}\right] \\
&= 1 - \left[\int_{\gamma_{\text{th}}/\varrho_{\text{S}}}^{\infty} f_{\mathcal{E}_u}(x)dx\right]\left[\int_{\gamma_{\text{th}}/\varrho_{\text{R}}}^{\infty} f_{\mathcal{E}'_w}(x)dx\right] \\
&= 1 - \left[1 - F_{\mathcal{E}_u}\left(\gamma_{\text{th}}/\varrho_{\text{S}}\right)\right]\left[1 - F_{\mathcal{E}'_w}\left(\gamma_{\text{th}}/\varrho_{\text{R}}\right)\right] \\
&= 1 - \left[\sum_{v=1}^{M} (-1)^v \binom{M}{v} \sum_{l_1=0}^{L-1} \sum_{k_1=1}^{m_{\text{SR}}} \cdots \sum_{l_v=0}^{L-1} \sum_{k_v=1}^{m_{\text{SR}}} \prod_{p=1}^{v} \Xi_{k_p} \left(\frac{\gamma_{\text{th}}}{\varrho_{\text{S}}}\right)^{A_1} e^{-\frac{A_2\gamma_{\text{th}}}{\varrho_{\text{S}}}}\right] \\
&\quad \times \left[\sum_{v'=1}^{M} (-1)^{v'} \binom{M}{v'} \sum_{l'_1=0}^{L-1} \sum_{k'_1=1}^{m_{\text{RD}}} \cdots \sum_{l'_{v'}=0}^{L-1} \sum_{k'_{v'}=1}^{m_{\text{RD}}} \prod_{p'=1}^{v'} \Xi'_{k'_{p'}} \left(\frac{\gamma_{\text{th}}}{\varrho_{\text{R}}}\right)^{A_3} e^{-\frac{A_4\gamma_{\text{th}}}{\varrho_{\text{R}}}}\right].
\end{aligned} \tag{19}$$

In the special case of $L = 1$, $m_{\text{SR}} = m_{\text{RD}} = 1$, $\varrho_{\text{S}} = \varrho_{\text{R}} = \varrho$, and $\Phi_{\text{SR},0} = \Phi_{\text{RD},0} = \Phi$, (19) reduces to

$$P_{\text{out}} = 1 - \left[1 - \left(1 - \exp\left(-\frac{\gamma_{\text{th}}}{\varrho\Phi}\right)\right)^M\right]^2, \tag{20}$$

which indicates that the outage probability decreases monotonously with the number of antennas M.

C. Optimal Power Allocation

In this subsection, we will find the optimal power allocation between the source and relay, which minimizes the outage probability for the aforementioned systems. We assume that the source and relay use $E_{b,\text{S}} = \zeta E_b$ and $E_{b,\text{R}} = (1-\zeta)E_b$ for their transmissions, respectively, where E_b is the transmitted bit energy for the whole relay system and $0 < \zeta < 1$. Recollect that $\varrho_{\text{S}} = \frac{E_{b,\text{S}}}{N_0/2}$ and $\varrho_{\text{R}} = \frac{E_{b,\text{R}}}{N_0/2}$. Thus, we have

$$\varrho_{\text{S}} = \zeta\,\varrho_{\text{tot}}\,, \tag{21a}$$

$$\varrho_{\text{R}} = (1-\zeta)\,\varrho_{\text{tot}} \tag{21b}$$

where $\varrho_{\text{tot}} = \frac{E_b}{N_0/2}$ is the total transmitted SNR.

$$\mathcal{J}_2 = M \sum_{l=0}^{L-1} \sum_{k=1}^{m_{\rm SR}} \Delta(l,k,m_{\rm SR},\{\Phi_{{\rm SR},\ell}\}_{\ell=0}^{L-1}) \Bigg\{ \exp\!\left(-\frac{\gamma_{\rm th}}{\Phi_{{\rm SR},l}\,\varrho_{\rm S}}\right) \sum_{c=0}^{k-1} \frac{1}{c!} \left(\frac{\gamma_{\rm th}}{\Phi_{{\rm SR},l}\,\varrho_{\rm S}}\right)^{c} + \frac{1}{\Phi_{{\rm SR},l}^{k}(k-1)!}$$
$$\times \Bigg[\sum_{v=1}^{M-1} (-1)^{v} \binom{M-1}{v} \sum_{l_1=0}^{L-1} \sum_{k_1=1}^{m_{\rm SR}} \cdots \sum_{l_v=0}^{L-1} \sum_{k_v=1}^{m_{\rm SR}} \prod_{p=1}^{v} \Xi_{k_p} \left(A_1+k, \frac{\gamma_{\rm th}}{\varrho_{\rm S}}\left(A_2+\frac{1}{\Phi_{{\rm SR},l}}\right)\right) \left(A_2+\frac{1}{\Phi_{{\rm SR},l}}\right)^{-A_1-k}$$
$$+ 2\sum_{v'=1}^{M} (-1)^{v'} \binom{M}{v'} \sum_{l'_1=0}^{L-1} \sum_{k'_1=1}^{m_{\rm RD}} \cdots \sum_{l'_{v'}=0}^{L-1} \sum_{k'_{v'}=1}^{m_{\rm RD}} \prod_{p'=1}^{v'} \Xi'_{k'_{p'}} \left(\frac{\gamma_{\rm th}}{\varrho_{\rm S}}\right)^{k} \left(\frac{\gamma_{\rm th}}{\varrho_{\rm R}}\right)^{A_3} \sqrt{A_4 \Phi_{{\rm SR},l} \frac{\varrho_{\rm S}}{\varrho_{\rm R}} \left(1+\frac{1}{\gamma_{\rm th}}\right)} \exp\!\left(-\frac{A_4\gamma_{\rm th}}{\varrho_{\rm R}} - \frac{\gamma_{\rm th}}{\Phi_{{\rm SR},l}\,\varrho_{\rm S}}\right)$$
$$\times \sum_{j_1=0}^{A_3} \binom{A_3}{j_1} \left[\frac{\varrho_{\rm R}}{A_4\Phi_{{\rm SR},l}\,\varrho_{\rm S}}\left(1+\frac{1}{\gamma_{\rm th}}\right)\right]^{\frac{j_1}{2}} \sum_{j_2=0}^{k-1} \binom{k-1}{j_2} \left[A_4\Phi_{{\rm SR},l}\frac{\varrho_{\rm S}}{\varrho_{\rm R}}\left(1+\frac{1}{\gamma_{\rm th}}\right)\right]^{\frac{j_2}{2}} \mathcal{K}_{j_2-j_1+1}\!\left(2\sqrt{\frac{A_4\gamma_{\rm th}(\gamma_{\rm th}+1)}{\Phi_{{\rm SR},l}\,\varrho_{\rm S}\,\varrho_{\rm R}}}\right)$$
$$+ 2\sum_{v=1}^{M-1}\sum_{v'=1}^{M} (-1)^{v+v'} \binom{M-1}{v}\binom{M}{v'} \sum_{l_1=0}^{L-1}\sum_{l'_1=0}^{L-1}\sum_{k_1=1}^{m_{\rm SR}}\sum_{k'_1=1}^{m_{\rm RD}} \cdots \sum_{l_v=0}^{L-1}\sum_{l'_{v'}=0}^{L-1}\sum_{k_v=1}^{m_{\rm SR}}\sum_{k'_{v'}=1}^{m_{\rm RD}} \prod_{p=1}^{v}\prod_{p'=1}^{v'} \Xi_{k_p}\Xi'_{k'_{p'}} \left(\frac{\gamma_{\rm th}}{\varrho_{\rm R}}\right)^{A_3} \left(\frac{\gamma_{\rm th}}{\varrho_{\rm S}}\right)^{A_1+k}$$
$$\times \sqrt{\frac{A_4\varrho_{\rm S}}{\varrho_{\rm R}}\left(\frac{1+1/\gamma_{\rm th}}{A_2+1/\Phi_{{\rm SR},l}}\right)} \exp\!\left(-\frac{A_4\gamma_{\rm th}}{\varrho_{\rm R}} - \frac{\gamma_{\rm th}}{\varrho_{\rm S}}\left(A_2+\frac{1}{\Phi_{{\rm SR},l}}\right)\right) \sum_{j_3=0}^{A_3} \binom{A_3}{j_3} \left[\frac{\varrho_{\rm R}}{A_4\varrho_{\rm S}}\left(A_2+\frac{1}{\Phi_{{\rm SR},l}}\right)\left(1+\frac{1}{\gamma_{\rm th}}\right)\right]^{\frac{j_3}{2}}$$
$$\times \sum_{j_4=0}^{A_1+k-1} \binom{A_1+k-1}{j_4} \left[\frac{A_4\varrho_{\rm S}}{\varrho_{\rm R}}\left(\frac{1+1/\gamma_{\rm th}}{A_2+1/\Phi_{{\rm SR},l}}\right)\right]^{\frac{j_4}{2}} \mathcal{K}_{j_4-j_3+1}\!\left(2\sqrt{\left(A_2+\frac{1}{\Phi_{{\rm SR},l}}\right)\frac{A_4\gamma_{\rm th}(\gamma_{\rm th}+1)}{\varrho_{\rm S}\,\varrho_{\rm R}}}\right)\Bigg]\Bigg\}. \tag{16}$$

1) AF System: From (13), it is clear that maximizing the end-to-end SNR, γ, results in minimizing the outage probability of the AF system. Our aim is then to derive the optimal ζ, which maximizes γ in (12). Substituting (21) into (12) and letting the derivative of (12) with respect to ζ equal zero, we obtain the optimal ζ as

$$\zeta_{\rm opt} = \begin{cases} \dfrac{1+\varrho_{\rm tot}\,\mathcal{E}'_w - \sqrt{(1+\varrho_{\rm tot}\,\mathcal{E}'_w)\,(1+\varrho_{\rm tot}\,\mathcal{E}_u)}}{\varrho_{\rm tot}\,(\mathcal{E}'_w - \mathcal{E}_u)}, & \mathcal{E}_u \neq \mathcal{E}'_w \\ 0.5, & \mathcal{E}_u = \mathcal{E}'_w. \end{cases} \tag{22}$$

Note that: 1) when $\mathcal{E}_u > \mathcal{E}'_w$, $1+\varrho_{\rm tot}\,\mathcal{E}'_w < \sqrt{(1+\varrho_{\rm tot}\,\mathcal{E}'_w)\,(1+\varrho_{\rm tot}\,\mathcal{E}_u)} < 1+\varrho_{\rm tot}\,\mathcal{E}_u$; and 2) when $\mathcal{E}_u < \mathcal{E}'_w$, $1+\varrho_{\rm tot}\,\mathcal{E}_u < \sqrt{(1+\varrho_{\rm tot}\,\mathcal{E}'_w)\,(1+\varrho_{\rm tot}\,\mathcal{E}_u)} < 1+\varrho_{\rm tot}\,\mathcal{E}'_w$. Therefore, it is easily checked that $\zeta_{\rm opt}$ in (22) is always in the interval $(0,1)$. Recall that the relay knows the channel coefficients $\{\alpha_{{\rm SR},u,l}\}_{l=0}^{L-1}$ and $\{\alpha_{{\rm RD},w,l}\}_{l=0}^{L-1}$. Hence, $\zeta_{\rm opt}$ in (22) can be readily calculated at the relay, and transmitted to the source through a noiseless feedback link.

2) DTF System: It is seen from (19) that the outage probability of the DTF system can be minimized by maximizing the term $\texttt{min}(\gamma_{\rm SR},\gamma_{\rm RD})$. Since $\gamma_{\rm SR}$ and $\gamma_{\rm RD}$ in (18) are monotonically increasing functions of $\varrho_{\rm S}$ and $\varrho_{\rm R}$ in (21), respectively, the optimal ζ which maximizes $\texttt{min}(\gamma_{\rm SR},\gamma_{\rm RD})$ can be found by substituting (21) into (18), and equating $\gamma_{\rm SR}$ and $\gamma_{\rm RD}$ in (18). This optimal ζ is obtained as

$$\zeta_{\rm opt} = \left(1+\frac{\mathcal{E}_u}{\mathcal{E}'_w}\right)^{-1}, \tag{23}$$

which does not depend on $\varrho_{\rm tot}$, unlike (22), and is always in the interval $(0,1)$ due to the fact that $0 < \mathcal{E}_u/\mathcal{E}'_w < \infty$. It can be realized at the relay and source in the same way as in the AF case. In Section VI, it will be shown that under the same energy constraint, i.e., $E_{b,{\rm S}} + E_{b,{\rm R}} = E_b$, the AF and DTF systems with optimal power allocation have superior outage performance compared to those with equal power allocation, respectively.

IV. Dual-Hop UWB Systems Using the Best Single-Antenna Relay

In these systems (see Fig. 1(b)), it is assumed that each available single-antenna relay has partial knowledge of its own channels towards the source and the destination, i.e., the q-th relay knows the channel coefficients $\{\alpha_{{\rm S}q,l}\}_{l=0}^{L-1}$ and $\{\alpha_{q{\rm D},l}\}_{l=0}^{L-1}$, where $L < L_t$. Based on this assumption, only the "best" relay is chosen to be active among all Q potential relays.[7] Details of the protocol for such selection can be found in [18], [49]. In what follows, we describe AF and DTF relaying schemes for such systems.

A. Amplify-and-Forward Relaying

In the AF relaying scheme, the data transmission from the source to the best relay can be described by (5)-(7), where the subscript R is replaced by the index of this relay, denoted as $q^\star$, and the antenna index is dropped. Meanwhile, the data transmission from the best relay to the destination can be described by (8)-(11) with the same modifications as before. Let us denote $\mathcal{E}_q = \sum_{l=0}^{L-1} \alpha_{{\rm S}q,l}^2$ and $\mathcal{E}'_q = \sum_{l=0}^{L-1} \alpha_{q{\rm D},l}^2$. The CDF and PDF of $\mathcal{E}_q$ can be written as (67) and (68), respectively, where the subscript R is replaced by the index q. Similarly, the CDF and PDF of $\mathcal{E}'_q$ are obtained as these two equations, respectively, both with $m_{\rm SR}$ being replaced by $m_{q{\rm D}}$, and $\Phi_{{\rm SR},\ell}$ (and

[7] We limit our discussion on such selection to *proactive* selection [18]. *Proactive* means that the relay selection is performed prior to the source transmission.

$\Phi_{\mathrm{SR},l}$) being replaced by $\Phi_{q\mathrm{D},\ell}$ (and $\Phi_{q\mathrm{D},l}$). Now the best relay can be represented by its index:

$$q^\star = \arg \max_{q\in\{1,2,\ldots,Q\}} \gamma_q \tag{24}$$

where $\gamma_q = \frac{\varrho_\mathrm{S}\,\mathcal{E}_q\,\varrho_q\,\mathcal{E}'_q}{\varrho_\mathrm{S}\,\mathcal{E}_q+\varrho_q\,\mathcal{E}'_q+1}$ is the overall end-to-end SNR corresponding to the q-th relay, and $\varrho_q = \frac{E_{b,q}}{N_0/2}$ is the transmitted SNR at this relay. From (13) and (24), we can derive the end-to-end SNR outage probability for the AF relaying scheme as follows:

$$\begin{aligned} P_\mathrm{out} &= \Pr\left[\gamma_{q^\star} \le \gamma_\mathrm{th}\right] \\ &= \Pr\left[\max_{q\in\{1,2,\ldots,Q\}} \gamma_q \le \gamma_\mathrm{th}\right] \\ &= \prod_{q=1}^{Q} \Pr\left[\frac{\varrho_\mathrm{S}\,\mathcal{E}_q\,\varrho_q\,\mathcal{E}'_q}{\varrho_\mathrm{S}\,\mathcal{E}_q+\varrho_q\,\mathcal{E}'_q+1} \le \gamma_\mathrm{th}\right] \end{aligned} \tag{25}$$

where

$$\begin{aligned} &\Pr\left[\frac{\varrho_\mathrm{S}\,\mathcal{E}_q\,\varrho_q\,\mathcal{E}'_q}{\varrho_\mathrm{S}\,\mathcal{E}_q+\varrho_q\,\mathcal{E}'_q+1} \le \gamma_\mathrm{th}\right] \\ &= \int_0^{\frac{\gamma_\mathrm{th}}{\varrho_\mathrm{S}}} f_{\mathcal{E}_q}(x)\,dx + \int_{\frac{\gamma_\mathrm{th}}{\varrho_\mathrm{S}}}^{\infty} F_{\mathcal{E}'_q}\!\left(\frac{\gamma_\mathrm{th}(\varrho_\mathrm{S}\,x+1)}{\varrho_\mathrm{S}\varrho_q\,x-\varrho_q\gamma_\mathrm{th}}\right) f_{\mathcal{E}_q}(x)\,dx \\ &= 1 - 2\sum_{l=0}^{L-1}\sum_{k=1}^{m_{\mathrm{S}q}} \Delta(l,k,m_{\mathrm{S}q},\{\Phi_{\mathrm{S}q,\ell}\}_{\ell=0}^{L-1}) \\ &\times \sum_{l'=0}^{L-1}\sum_{k'=1}^{m_{q\mathrm{D}}} \Delta(l',k',m_{q\mathrm{D}},\{\Phi_{q\mathrm{D},\ell'}\}_{\ell'=0}^{L-1}) \\ &\times \frac{{\gamma_\mathrm{th}}^k}{(k-1)!\;\left(\Phi_{\mathrm{S}q,l}\,\varrho_\mathrm{S}\right)^k} \sqrt{\frac{\Phi_{\mathrm{S}q,l}\,\varrho_\mathrm{S}}{\Phi_{q\mathrm{D},l'}\,\varrho_q}\left(1+\frac{1}{\gamma_\mathrm{th}}\right)} \\ &\times \exp\!\left(-\gamma_\mathrm{th}\left(\frac{1}{\Phi_{\mathrm{S}q,l}\,\varrho_\mathrm{S}}+\frac{1}{\Phi_{q\mathrm{D},l'}\,\varrho_q}\right)\right) \sum_{i_1=0}^{k'-1} \frac{{\gamma_\mathrm{th}}^{i_1}}{i_1!\;\left(\Phi_{q\mathrm{D},l'}\,\varrho_q\right)^{i_1}} \\ &\times \sum_{i_2=0}^{i_1}\binom{i_1}{i_2}\left[\frac{\Phi_{q\mathrm{D},l'}\,\varrho_q}{\Phi_{\mathrm{S}q,l}\,\varrho_\mathrm{S}}\left(1+\frac{1}{\gamma_\mathrm{th}}\right)\right]^{\frac{i_2}{2}} \sum_{i_3=0}^{k-1}\binom{k-1}{i_3} \\ &\times \left[\frac{\Phi_{\mathrm{S}q,l}\,\varrho_\mathrm{S}}{\Phi_{q\mathrm{D},l'}\,\varrho_q}\left(1+\frac{1}{\gamma_\mathrm{th}}\right)\right]^{\frac{i_3}{2}} \mathcal{K}_{i_3-i_2+1}\!\left(2\sqrt{\frac{\gamma_\mathrm{th}(1+\gamma_\mathrm{th})}{\Phi_{\mathrm{S}q,l}\,\varrho_\mathrm{S}\,\Phi_{q\mathrm{D},l'}\,\varrho_q}}\right). \end{aligned} \tag{26}$$

The first and second equalities in (26) are obtained by following (14) and the same analysis approach as in [50, Subsection III-A], respectively.

B. Detect-and-Forward Relaying

Let $q^\diamond$ be the index of the best relay for the DTF relaying scheme. The description of the data transmissions from the source to the $q^\diamond$-th relay and from this relay to the destination can be done as in the preceding scheme except that $q^\star$ is substituted by $q^\diamond$, and $\bar{z}_{q^\diamond}$ is substituted by $\hat{b}_{q^\diamond} = \mathtt{sign}(z_{q^\diamond})$ since the relay makes a hard decision on $z_{q^\diamond}$. The best relay can be represented by its index:

$$q^\diamond = \arg \max_{q\in\{1,2,\ldots,Q\}} \left[\mathtt{min}(\gamma_{\mathrm{S}q},\gamma_{q\mathrm{D}})\right] \tag{27}$$

where $\gamma_{\mathrm{S}q} = \mathcal{E}_q\,\varrho_\mathrm{S}$ and $\gamma_{q\mathrm{D}} = \mathcal{E}'_q\,\varrho_q$ are the received SNRs for the first and second hops, respectively, both corresponding to the q-th relay. Consequently, we obtain the end-to-end SNR outage probability as

$$\begin{aligned} P_\mathrm{out} &= \Pr\left[\gamma_{q^\diamond} \le \gamma_\mathrm{th}\right] \\ &= \Pr\left[\max_{q\in\{1,2,\ldots,Q\}} \left[\mathtt{min}(\gamma_{\mathrm{S}q},\gamma_{q\mathrm{D}})\right] \le \gamma_\mathrm{th}\right] \\ &= \prod_{q=1}^{Q} \Pr\left[\mathtt{min}(\gamma_{\mathrm{S}q},\gamma_{q\mathrm{D}}) \le \gamma_\mathrm{th}\right] \end{aligned} \tag{28}$$

where

$$\begin{aligned} &\Pr\left[\mathtt{min}(\gamma_{\mathrm{S}q},\gamma_{q\mathrm{D}}) \le \gamma_\mathrm{th}\right] \\ &= 1-\left[1-F_{\mathcal{E}_q}\;\gamma_\mathrm{th}/\varrho_\mathrm{S}\right)\left]\left[1-F_{\mathcal{E}'_q}\;\gamma_\mathrm{th}/\varrho_q\right)\right] \\ &= 1-\left[\sum_{l=0}^{L-1}\sum_{k=1}^{m_{\mathrm{S}q}} \Delta(l,k,m_{\mathrm{S}q},\{\Phi_{\mathrm{S}q,\ell}\}_{\ell=0}^{L-1}) \frac{\left(k,\frac{\gamma_\mathrm{th}}{\Phi_{\mathrm{S}q,l}\,\varrho_\mathrm{S}}\right)}{(k-1)!}\right] \\ &\quad\times\left[\sum_{l'=0}^{L-1}\sum_{k'=1}^{m_{q\mathrm{D}}} \Delta(l',k',m_{q\mathrm{D}},\{\Phi_{q\mathrm{D},\ell}\}_{\ell'=0}^{L-1}) \frac{\left(k',\frac{\gamma_\mathrm{th}}{\Phi_{q\mathrm{D},l'}\,\varrho_q}\right)}{(k'-1)!}\right] \end{aligned} \tag{29}$$

and the first equality in (29) is obtained by following (19).

C. Optimal Power Allocation

Since each available single-antenna relay in the above systems has partial knowledge of its own channels towards the source and the destination, the relay selection can be combined with the optimal power allocation between the source and relay, which is described as follows.

1) AF System: First, following the same procedure as in Subsection III-C.1, the optimal ζ which maximizes γ_q in (24) is obtained at the q-th relay as

$$\zeta_{\mathrm{opt},q} = \begin{cases} \dfrac{1+\varrho_\mathrm{tot}\,\mathcal{E}'_q-\sqrt{(1+\varrho_\mathrm{tot}\,\mathcal{E}'_q)\,(1+\varrho_\mathrm{tot}\,\mathcal{E}_q)}}{\varrho_\mathrm{tot}\,(\mathcal{E}'_q-\mathcal{E}_q)}, & \mathcal{E}_q \ne \mathcal{E}'_q \\ 0.5, & \mathcal{E}_q = \mathcal{E}'_q. \end{cases} \tag{30}$$

As in Subsection III-C.1, we can check that $0 < \zeta_{\mathrm{opt},q} < 1$. From (21) and (30), the end-to-end SNR $\gamma_{\mathrm{opt},q} = \frac{\zeta_{\mathrm{opt},q}\,(1-\zeta_{\mathrm{opt},q})\,\mathcal{E}_q\,\mathcal{E}'_q\,\varrho^2_\mathrm{tot}}{\zeta_{\mathrm{opt},q}\,\mathcal{E}_q\,\varrho_\mathrm{tot}+(1-\zeta_{\mathrm{opt},q})\,\mathcal{E}'_q\,\varrho_\mathrm{tot}+1}$ can be computed at the q-th relay. Only the relay with the largest value of this SNR is chosen as the active relay.[8] Finally, this relay sends its optimal ζ to the source via an error-free feedback channel.

2) DTF System: Initially, following the same procedure as in Subsection III-C.2, the optimal ζ which maximizes the term $\mathtt{min}(\gamma_{\mathrm{S}q},\gamma_{q\mathrm{D}})$ in (27) is obtained at the q-th relay as

$$\zeta_{\mathrm{opt},q} = \left(1+\frac{\mathcal{E}_q}{\mathcal{E}'_q}\right)^{-1}. \tag{31}$$

As in Subsection III-C.2, we can check that $0 < \zeta_{\mathrm{opt},q} < 1$. From (18), (21), and (31), either the received SNR for the first hop $\gamma_{\mathrm{S}q} = \zeta_{\mathrm{opt},q}\,\mathcal{E}_q\,\varrho_\mathrm{tot}$ or the one for the second hop $\gamma_{q\mathrm{D}} = (1-\zeta_{\mathrm{opt},q})\,\mathcal{E}'_q\,\varrho_\mathrm{tot}$ is then calculated at the q-th relay (because $\gamma_{\mathrm{S}q}$ and $\gamma_{q\mathrm{D}}$ are equal). The relay with the

[8] In practice, such relay selection can be realized using the protocol suggested in [49] with certain parameter modification.

largest value of the calculated SNR is chosen as the active relay. Lastly, the optimal ζ for this relay can be conveyed to the source through an error-free feedback channel. It is evident that the relay selection criteria with optimal power allocation are basically different from those described in Subsections IV-A and IV-B.

V. Extension to Two-Way Relaying

A. Two-Way UWB Relay Systems Using a Multiple-Antenna Relay with Antenna Selection

The system model is shown in Fig. 2(a), where the channels are assumed to be reciprocal.[9] For these systems, we follow the assumption of partial channel knowledge at the relay and the antenna selection criterion in Section III.

1) Amplify-and-Forward Relaying: As mentioned before, the antenna index u may or may not be equal to the antenna index w. First, we consider the case when $u \neq w$. Let $b^{[1]}$ and $b^{[2]}$ be the transmitted binary bits of the source and destination, respectively. For the first phase, the transmitted signal at the source can be modeled as (5) with b being replaced by $b^{[1]}$, and the transmitted signal at the destination can be modeled as (5) with b being replaced by $b^{[2]}$ and the subscript S being replaced by the subscript D. As in Subsection III-A, Rake reception is performed at the u-th antenna of the relay. The correlator output corresponding to the l-th finger is given by

$$y_{\mathrm{R},u,l}(i) = b^{[1]}\sqrt{E_{f,\mathrm{S}}}\alpha_{\mathrm{SR},u,l} + b^{[2]}\sqrt{E_{f,\mathrm{D}}}\alpha_{\mathrm{DR},u,l} + n_{\mathrm{R},u,l}(i); \quad l = 0,\ldots,L-1;\ i = 1,\ldots,N_f \tag{32}$$

where the second term is treated as noise. Hence, the Rake combining output can be written as $z_{\mathrm{R}}^{[1]} = \sum_{i=1}^{N_f}\sum_{l=0}^{L-1}\alpha_{\mathrm{SR},u,l}\, y_{\mathrm{R},u,l}(i)$. Meanwhile, additional Rake reception is performed at the w-th antenna of the relay. The correlator output is the same as (32) except that u is replaced by w and the first term is treated as noise instead. The corresponding Rake combining output is $z_{\mathrm{R}}^{[2]} = \sum_{i=1}^{N_f}\sum_{l=0}^{L-1}\alpha_{\mathrm{DR},w,l}\, y_{\mathrm{R},w,l}(i)$.[10]

In the second phase, the relay transmits $z_{\mathrm{R}}^{[1]}$ and $z_{\mathrm{R}}^{[2]}$ at the w-th and u-th antennas, respectively, as

$$x_{\mathrm{R},w}(t) = \bar{z}_{\mathrm{R}}^{[1]}\sqrt{\frac{E_{f,\mathrm{R}}^{[1]}}{\mathcal{E}'_w}}\sum_{i=1}^{N_f}\sum_{l=0}^{L-1}\alpha_{\mathrm{RD},w,L-1-l}\, g(t-(i+N_f-1)T_f - lT_g), \tag{33a}$$

$$x_{\mathrm{R},u}(t) = \bar{z}_{\mathrm{R}}^{[2]}\sqrt{\frac{E_{f,\mathrm{R}}^{[2]}}{\mathcal{E}_u}}\sum_{i=1}^{N_f}\sum_{l=0}^{L-1}\alpha_{\mathrm{RS},u,L-1-l}\, g(t-(i+N_f-1)T_f - lT_g) \tag{33b}$$

where $\bar{z}_{\mathrm{R}}^{[1]} = z_{\mathrm{R}}^{[1]}\Big/\sqrt{N_f\mathcal{E}_u B_1}$ with $B_1 = E_{b,\mathrm{S}}\mathcal{E}_u + E_{b,\mathrm{D}}\mathcal{I}^2/\mathcal{E}_u + N_0/2$ and $\mathcal{I} = \sum_{l=0}^{L-1}\alpha_{\mathrm{SR},u,l}\alpha_{\mathrm{DR},u,l}$, and $\bar{z}_{\mathrm{R}}^{[2]} = z_{\mathrm{R}}^{[2]}\Big/\sqrt{N_f\mathcal{E}'_w B_2}$ with $B_2 = E_{b,\mathrm{D}}\mathcal{E}'_w + E_{b,\mathrm{S}}\mathcal{I}'^2/\mathcal{E}'_w + N_0/2$ and $\mathcal{I}' = \sum_{l=0}^{L-1}\alpha_{\mathrm{SR},w,l}\alpha_{\mathrm{DR},w,l}$. In the above equation, $z_{\mathrm{R}}^{[1]}$ and $z_{\mathrm{R}}^{[2]}$ are normalized for the same reason as z_{R} in (8). Similar to (10), the received signal at the destination, after passing through the matched filter and sampling, which is used to form the decision variable for $b^{[1]}$ can be expressed as

$$\begin{aligned} y_{\mathrm{D},L-1}(i) = {} & \bar{z}_{\mathrm{R}}^{[1]}\sqrt{\frac{E_{f,\mathrm{R}}^{[1]}}{\mathcal{E}'_w}}\sum_{l=0}^{L-1}\alpha_{\mathrm{RD},w,l}^2 \\ & + \bar{z}_{\mathrm{R}}^{[2]}\sqrt{\frac{E_{f,\mathrm{R}}^{[2]}}{\mathcal{E}_u}}\sum_{l=0}^{L-1}\alpha_{\mathrm{RS},u,l}\alpha_{\mathrm{RD},w,l} \\ & + n_{\mathrm{D},L-1}(i);\ i = 1,\ldots,N_f. \end{aligned} \tag{34}$$

After some manipulations, we have

$$\begin{aligned} y_{\mathrm{D},L-1}(i) = {} & b^{[1]}\left[\sqrt{\frac{E_{b,\mathrm{S}}E_{f,\mathrm{R}}^{[1]}\mathcal{E}_u\,\mathcal{E}'_w}{B_1}} + \mathcal{I}'\mathcal{I}''\sqrt{\frac{E_{b,\mathrm{S}}E_{f,\mathrm{R}}^{[2]}}{\mathcal{E}_u\,\mathcal{E}'_w\,B_2}}\right] \\ & + b^{[2]}\left[\mathcal{I}\sqrt{\frac{E_{b,\mathrm{D}}E_{f,\mathrm{R}}^{[1]}\mathcal{E}'_w}{\mathcal{E}_u\,B_1}} + \mathcal{I}''\sqrt{\frac{E_{b,\mathrm{D}}E_{f,\mathrm{R}}^{[2]}\mathcal{E}'_w}{\mathcal{E}_u\,B_2}}\right] + n_{\mathrm{D},L-1}(i) \\ & + \sqrt{\frac{E_{f,\mathrm{R}}^{[1]}\mathcal{E}'_w}{N_f\mathcal{E}_u\,B_1}}\sum_{i=1}^{N_f}\sum_{l=0}^{L-1}\alpha_{\mathrm{SR},u,l}n_{\mathrm{R},u,l}(i) \\ & + \mathcal{I}''\sqrt{\frac{E_{f,\mathrm{R}}^{[2]}}{N_f\mathcal{E}_u\,\mathcal{E}'_w\,B_2}}\sum_{i=1}^{N_f}\sum_{l=0}^{L-1}\alpha_{\mathrm{DR},w,l}n_{\mathrm{R},w,l}(i) \end{aligned} \tag{35}$$

where $\mathcal{I}'' = \sum_{l=0}^{L-1}\alpha_{\mathrm{RS},u,l}\alpha_{\mathrm{RD},w,l}$. By assuming that $E_{f,\mathrm{R}}^{[1]}$, $E_{f,\mathrm{R}}^{[2]}$, $\{\alpha_{\mathrm{SR},u,l}\}_{l=0}^{L-1}$, $\{\alpha_{\mathrm{SR},w,l}\}_{l=0}^{L-1}$, $\{\alpha_{\mathrm{RD},u,l}\}_{l=0}^{L-1}$, and $\{\alpha_{\mathrm{RD},w,l}\}_{l=0}^{L-1}$ are known at the destination, the self-interference component, i.e., $b^{[2]}\left[\mathcal{I}\sqrt{\frac{E_{b,\mathrm{D}}E_{f,\mathrm{R}}^{[1]}\mathcal{E}'_w}{\mathcal{E}_u\,B_1}} + \mathcal{I}''\sqrt{\frac{E_{b,\mathrm{D}}E_{f,\mathrm{R}}^{[2]}\mathcal{E}'_w}{\mathcal{E}_u\,B_2}}\right]$, can be subtracted from $y_{\mathrm{D},L-1}(i)$ to obtain

$$\begin{aligned} \check{y}_{\mathrm{D},L-1}(i) = {} & b^{[1]}\left[\sqrt{\frac{E_{b,\mathrm{S}}E_{f,\mathrm{R}}^{[1]}\mathcal{E}_u\,\mathcal{E}'_w}{B_1}} + \mathcal{I}'\mathcal{I}''\sqrt{\frac{E_{b,\mathrm{S}}E_{f,\mathrm{R}}^{[2]}}{\mathcal{E}_u\,\mathcal{E}'_w\,B_2}}\right] \\ & + \sqrt{\frac{E_{f,\mathrm{R}}^{[1]}\mathcal{E}'_w}{N_f\mathcal{E}_u\,B_1}}\sum_{i=1}^{N_f}\sum_{l=0}^{L-1}\alpha_{\mathrm{SR},u,l}\,n_{\mathrm{R},u,l}(i) + n_{\mathrm{D},L-1}(i) \\ & + \mathcal{I}''\sqrt{\frac{E_{f,\mathrm{R}}^{[2]}}{N_f\mathcal{E}_u\,\mathcal{E}'_w\,B_2}}\sum_{i=1}^{N_f}\sum_{l=0}^{L-1}\alpha_{\mathrm{DR},w,l}\,n_{\mathrm{R},w,l}(i). \end{aligned} \tag{36}$$

Then, the decision variable for $b^{[1]}$ is given by

$$z_{\mathrm{D}} = \sum_{i=1}^{N_f}\check{y}_{\mathrm{D},L-1}(i). \tag{37}$$

[9] The experimental results in [51] show that the reciprocal theorem is indeed valid for a UWB multipath environment.

[10] Recollect that the relay knows $\{\alpha_{\mathrm{RD},w,l}\}_{l=0}^{L-1}$, and $\alpha_{\mathrm{DR},w,l}$ $\alpha_{\mathrm{RD},w,l}$ owing to the channel reciprocity assumed.

Through some tedious but straightforward calculations, we obtain the SNR of this decision variable as

$$\gamma^{[1]} = \frac{\varrho_{\rm S}\,\mathcal{E}_u\,\varrho_{\rm R}^{[1]}\,\mathcal{E}'_w + \mathcal{S}}{\varrho_{\rm S}\,\mathcal{E}_u + \varrho_{\rm R}^{[1]}\,\mathcal{E}'_w + 1 + \mathcal{N}} \tag{38}$$

where $\mathcal{S} = \varrho_{\rm S}\,\varrho_{\rm R}^{[2]}\left(\frac{\varrho_{\rm S}\mathcal{E}_u^2+\varrho_{\rm D}\mathcal{I}^{\,2}+\mathcal{E}_u}{\varrho_{\rm D}\mathcal{E}_w'^2+\varrho_{\rm S}\mathcal{I}'^2+\mathcal{E}'_w}\right)\left(\frac{\mathcal{I}'\mathcal{I}''}{\mathcal{E}_u}\right)^2$, $\mathcal{N} = \frac{\varrho_{\rm D}}{\mathcal{E}_u}\mathcal{I}^{\,2} + \varrho_{\rm R}^{[2]}\mathcal{E}'_w\left(\frac{\varrho_{\rm S}\mathcal{E}_u^2+\varrho_{\rm D}\mathcal{I}^{\,2}+\mathcal{E}_u}{\varrho_{\rm D}\mathcal{E}_w'^2+\varrho_{\rm S}\mathcal{I}'^2+\mathcal{E}'_w}\right)\left(\frac{\mathcal{I}''}{\mathcal{E}_u}\right)^2$, $\varrho_{\rm D} = \frac{E_{b,{\rm D}}}{N_0/2}$ is the transmitted SNR at the destination, and $\varrho_{\rm R}^{[1]} = \frac{E_{b,{\rm R}}^{[1]}}{N_0/2}$ and $\varrho_{\rm R}^{[2]} = \frac{E_{b,{\rm R}}^{[2]}}{N_0/2}$ are the transmitted SNRs (corresponding to $b^{[1]}$ and $b^{[2]}$, respectively) at the relay. Similarly, given that the source knows $E_{f,{\rm R}}^{[1]}$, $E_{f,{\rm R}}^{[2]}$, $\{\alpha_{{\rm DR},u,l}\}_{l=0}^{L-1}$, $\{\alpha_{{\rm DR},w,l}\}_{l=0}^{L-1}$, $\{\alpha_{{\rm RS},u,l}\}_{l=0}^{L-1}$, and $\{\alpha_{{\rm RS},w,l}\}_{l=0}^{L-1}$, the SNR of the decision variable for $b^{[2]}$ is

$$\gamma^{[2]} = \frac{\varrho_{\rm R}^{[2]}\,\mathcal{E}_u\,\varrho_{\rm D}\,\mathcal{E}'_w + \mathcal{S}'}{\varrho_{\rm R}^{[2]}\,\mathcal{E}_u + \varrho_{\rm D}\,\mathcal{E}'_w + 1 + \mathcal{N}'} \tag{39}$$

where $\mathcal{S}' = \varrho_{\rm R}^{[1]}\varrho_{\rm D}\left(\frac{\varrho_{\rm D}\mathcal{E}_w'^2+\varrho_{\rm S}\mathcal{I}'^2+\mathcal{E}'_w}{\varrho_{\rm S}\mathcal{E}_u^2+\varrho_{\rm D}\mathcal{I}^{\,2}+\mathcal{E}_u}\right)\left(\frac{\mathcal{I}\mathcal{I}''}{\mathcal{E}'_w}\right)^2$ and $\mathcal{N}' = \frac{\varrho_{\rm S}}{\mathcal{E}'_w}\mathcal{I}'^2 + \varrho_{\rm R}^{[1]}\mathcal{E}_u\left(\frac{\varrho_{\rm D}\mathcal{E}_w'^2+\varrho_{\rm S}\mathcal{I}'^2+\mathcal{E}'_w}{\varrho_{\rm S}\mathcal{E}_u^2+\varrho_{\rm D}\mathcal{I}^{\,2}+\mathcal{E}_u}\right)\left(\frac{\mathcal{I}''}{\mathcal{E}'_w}\right)^2$.

It is quite straightforward to extend the above analysis to the case when $u = w$. The difference from the above-described case of $u \neq w$ is that the Rake combining outputs $z_{\rm R}^{[1]}$ and $z_{\rm R}^{[2]}$ are derived from the same antenna of the relay in the first phase, and then transmitted at this antenna in the second phase as the sum of all the terms on the right-hand sides of (33a) and (33b). Accordingly, we have $\mathcal{I}'' = \mathcal{I}' = \mathcal{I}$ in (33)-(39).

As in [52], we assume that, in the two-way AF system, an outage occurs when both $\gamma^{[1]}$ and $\gamma^{[2]}$ fall below the prespecified SNR threshold $\gamma_{\rm th}$. The outage probability is thus written as

$$P_{\rm out} = \Pr\Big[\mathtt{max}(\gamma^{[1]}, \gamma^{[2]}) \leq \gamma_{\rm th}\Big]. \tag{40}$$

Unfortunately, it is difficult, if not impossible, to find the closed-form expression of (40). In this case, the outage probability is determined by means of simulations.

2) Detect-and-Forward Relaying: Let us first consider the case when $u \neq w$. For the first phase, the description of the data transmissions from the source and destination to the relay can be done as in the two-way AF relaying scheme. However, the relay makes hard decisions on the Rake combining outputs $z_{\rm R}^{[1]}$ and $z_{\rm R}^{[1]}$, yielding $\hat{b}_{\rm R}^{[1]} = \mathtt{sign}(z_{\rm R}^{[1]})$ and $\hat{b}_{\rm R}^{[2]} = \mathtt{sign}(z_{\rm R}^{[2]})$. For the second phase, the transmitted signals at the relay and the received signal at the destination can be expressed, respectively, as (33) and (34), both with $\bar{z}_{\rm R}^{[1]}$ being replaced by $\hat{b}_{\rm R}^{[1]}$ and $\bar{z}_{\rm R}^{[2]}$ being replaced by $\hat{b}_{\rm R}^{[2]}$. Using the assumption that the destination knows $E_{f,{\rm R}}^{[2]}$, $\{\alpha_{{\rm SR},u,l}\}_{l=0}^{L-1}$, and $\{\alpha_{{\rm RD},w,l}\}_{l=0}^{L-1}$, the interference term $\hat{b}_{\rm R}^{[2]}\sqrt{E_{f,{\rm R}}^{[2]}/\mathcal{E}_u}\sum_{l=0}^{L-1}\alpha_{{\rm RS},u,l}\alpha_{{\rm RD},w,l}$ can be subtracted from $y_{{\rm D},L-1}(i)$ or not depending on whether the relay detects $b^{[2]}$ correctly.[11] More precisely, after generating $b^{[2]}\sqrt{E_{f,{\rm R}}^{[2]}/\mathcal{E}_u}\sum_{l=0}^{L-1}\alpha_{{\rm RS},u,l}\alpha_{{\rm RD},w,l}$ and subtracting it from $y_{{\rm D},L-1}(i)$, the destination obtains

$$\check{y}_{{\rm D},L-1}(i) = \begin{cases} \hat{b}_{\rm R}^{[1]}\sqrt{\frac{E_{f,{\rm R}}^{[1]}}{\mathcal{E}'_w}}\sum_{l=0}^{L-1}\alpha_{{\rm RD},w,l}^2 + n_{{\rm D},L-1}(i),\ \hat{b}_{\rm R}^{[2]} = b^{[2]} \\ \hat{b}_{\rm R}^{[1]}\sqrt{\frac{E_{f,{\rm R}}^{[1]}}{\mathcal{E}'_w}}\sum_{l=0}^{L-1}\alpha_{{\rm RD},w,l}^2 + \left(\hat{b}_{\rm R}^{[2]} - b^{[2]}\right)\sqrt{\frac{E_{f,{\rm R}}^{[2]}}{\mathcal{E}_u}} \\ \times\sum_{l=0}^{L-1}\alpha_{{\rm RS},u,l}\alpha_{{\rm RD},w,l} + n_{{\rm D},L-1}(i),\ \hat{b}_{\rm R}^{[2]} \neq b^{[2]}. \end{cases} \tag{41}$$

Finally, the decision variable for $b^{[1]}$ is given by (37). It is straightforward to show that the received SNRs for the S→R link and R→D link are, respectively,

$$\gamma_{\rm SR}^{[1]} = \frac{\varrho_{\rm S}\,\mathcal{E}_u}{1 + \frac{\varrho_{\rm D}\mathcal{I}^{\,2}}{\mathcal{E}_u}}, \tag{42a}$$

$$\gamma_{\rm RD}^{[1]} = \begin{cases} \varrho_{\rm R}^{[1]}\mathcal{E}'_w\,, & \hat{b}_{\rm R}^{[1]} = b^{[1]} \\ \dfrac{\varrho_{\rm R}^{[1]}\mathcal{E}'_w}{1 + \frac{4\varrho_{\rm R}^{[2]}\mathcal{I}'^2}{\mathcal{E}_u}}, & \hat{b}_{\rm R}^{[1]} \neq b^{[1]}. \end{cases} \tag{42b}$$

Likewise, given that the source knows $E_{f,{\rm R}}^{[1]}$, $\{\alpha_{{\rm DR},w,l}\}_{l=0}^{L-1}$, and $\{\alpha_{{\rm RS},u,l}\}_{l=0}^{L-1}$, the received SNRs for the D→R link and R→S link are obtained, respectively, as

$$\gamma_{\rm DR}^{[2]} = \frac{\varrho_{\rm D}\,\mathcal{E}'_w}{1 + \frac{\varrho_{\rm S}\mathcal{I}'^2}{\mathcal{E}'_w}}, \tag{43a}$$

$$\gamma_{\rm RS}^{[2]} = \begin{cases} \varrho_{\rm R}^{[2]}\mathcal{E}_u\,, & \hat{b}_{\rm R}^{[2]} = b^{[2]} \\ \dfrac{\varrho_{\rm R}^{[2]}\mathcal{E}_u}{1 + \frac{4\varrho_{\rm R}^{[1]}\mathcal{I}'^2}{\mathcal{E}'_w}}, & \hat{b}_{\rm R}^{[2]} \neq b^{[2]}. \end{cases} \tag{43b}$$

The extension of the above analysis to the case when $u = w$ is fairly straightforward. The difference from the above-described case of $u \neq w$ is that the Rake combining outputs $z_{\rm R}^{[1]}$ and $z_{\rm R}^{[2]}$ are derived from the same antenna of the relay in the first phase, and then transmitted at this antenna in the second phase as the sum of all the terms on the right-hand sides of (33a) and (33b), both with $\bar{z}_{\rm R}^{[1]}$ being replaced by $\hat{b}_{\rm R}^{[1]}$ and $\bar{z}_{\rm R}^{[2]}$ being replaced by $\hat{b}_{\rm R}^{[2]}$. Therefore, we have $\mathcal{I}'' = \mathcal{I}' = \mathcal{I}$ in (42) and (43).

Analogous to (40), we have

$$P_{\rm out} = \Pr\Big[\mathtt{max}\left(\mathtt{min}(\gamma_{\rm SR}^{[1]}, \gamma_{\rm RD}^{[1]}), \mathtt{min}(\gamma_{\rm DR}^{[2]}, \gamma_{\rm RS}^{[2]})\right) \leq \gamma_{\rm th}\Big]. \tag{44}$$

Since the outage probability in (44) is not available in closed-form, it is computed via simulations.

3) Optimal Power Allocation: In what follows, we assume that $\varrho_{\rm S} = \varrho_{\rm D} = \zeta\,\varrho_{\rm tot}$ and $\varrho_{\rm R}^{[1]} = \varrho_{\rm R}^{[2]} = (1-\zeta)\,\varrho_{\rm tot}$. We first derive the optimal power allocation between the source and relay, which minimizes the outage probability for the two-way AF system. For analytical tractability, we assume that $\varrho_{\rm tot}$ is large enough such that $\varrho_{\rm S}\mathcal{E}_u^2 + \varrho_{\rm D}\mathcal{I}^{\,2} + \mathcal{E}_u \approx \varrho_{\rm S}\mathcal{E}_u^2 + \varrho_{\rm D}\mathcal{I}^{\,2}$ and $\varrho_{\rm D}\mathcal{E}_w'^2 + \varrho_{\rm S}\mathcal{I}'^2 + \mathcal{E}'_w \approx \varrho_{\rm D}\mathcal{E}_w'^2 + \varrho_{\rm S}\mathcal{I}'^2$. Hence, the SNR $\gamma^{[1]}$ in (38) can be

[11] Different from most work on two-way relaying [26]–[28], we do *not* assume that the relay can detect $b^{[1]}$ and $b^{[2]}$ without errors.

approximated as

$$\gamma^{[1]} \approx \frac{C_3(1-\zeta)\zeta}{C_2\zeta + C_1} \triangleq \gamma_{\text{ap}}^{[1]} \tag{45}$$

where $C_1 = \varrho_{\text{tot}}\,\mathcal{E}'_w\left[1+\left(\frac{\mathcal{E}_u^2+\mathcal{I}^{\,2}}{\mathcal{E}_w'^2+\mathcal{I}'^2}\right)\left(\frac{\mathcal{I}''}{\mathcal{E}_u}\right)^2\right]+1$, $C_2 = \varrho_{\text{tot}}\left[\mathcal{E}_u+\frac{\mathcal{I}^2}{\mathcal{E}_u}-\mathcal{E}'_w-\mathcal{E}'_w\left(\frac{\mathcal{E}_u^2+\mathcal{I}^{\,2}}{\mathcal{E}_w'^2+\mathcal{I}'^2}\right)\left(\frac{\mathcal{I}''}{\mathcal{E}_u}\right)^2\right]$, and $C_3 = \varrho_{\text{tot}}^2\left[\mathcal{E}_u\,\mathcal{E}'_w+\left(\frac{\mathcal{E}_u^2+\mathcal{I}^{\,2}}{\mathcal{E}_w'^2+\mathcal{I}'^2}\right)\left(\frac{\mathcal{I}'\mathcal{I}''}{\mathcal{E}_u}\right)^2\right]$. Let $\zeta_{\text{ap}}^{[1]}$ be the optimal ζ, which maximizes $\gamma_{\text{ap}}^{[1]}$ in (45). It is easy to show that

$$\zeta_{\text{ap}}^{[1]} = \begin{cases} \dfrac{\sqrt{C_1\,(C_1+C_2)}-C_1}{C_2}, & C_2 \neq 0 \\ 0.5\,, & C_2 = 0. \end{cases} \tag{46}$$

Since $C_1 + C_2 > 1$, it can be verified that $\zeta_{\text{ap}}^{[1]}$ in (46) is always in the interval $(0,1)$. Similarly, the SNR $\gamma^{[2]}$ in (39) can be approximated as

$$\gamma^{[2]} \approx \frac{C'_3(1-\zeta)\zeta}{C'_2\zeta + C'_1} \triangleq \gamma_{\text{ap}}^{[2]} \tag{47}$$

where $C'_1 = \varrho_{\text{tot}}\,\mathcal{E}_u\left[1+\left(\frac{\mathcal{E}_w'^2+\mathcal{I}'^2}{\mathcal{E}_u^2+\mathcal{I}^{\,2}}\right)\left(\frac{\mathcal{I}''}{\mathcal{E}'_w}\right)^2\right]+1$, $C'_2 = \varrho_{\text{tot}}\left[\mathcal{E}'_w+\frac{\mathcal{I}'^2}{\mathcal{E}'_w}-\mathcal{E}_u-\mathcal{E}_u\left(\frac{\mathcal{E}_w'^2+\mathcal{I}'^2}{\mathcal{E}_u^2+\mathcal{I}^{\,2}}\right)\left(\frac{\mathcal{I}''}{\mathcal{E}'_w}\right)^2\right]$, and $C'_3 = \varrho_{\text{tot}}^2\left[\mathcal{E}_u\,\mathcal{E}'_w+\left(\frac{\mathcal{E}_w'^2+\mathcal{I}'^2}{\mathcal{E}_u^2+\mathcal{I}^{\,2}}\right)\left(\frac{\mathcal{I}\mathcal{I}''}{\mathcal{E}'_w}\right)^2\right]$. The optimal ζ, which maximizes $\gamma_{\text{ap}}^{[2]}$ in (47), is given by

$$\zeta_{\text{ap}}^{[2]} = \begin{cases} \dfrac{\sqrt{C'_1\,(C'_1+C'_2)}-C'_1}{C'_2}, & C'_2 \neq 0 \\ 0.5\,, & C'_2 = 0. \end{cases} \tag{48}$$

It is clear that $\gamma_{\text{ap}}^{[1]}$ in (45) and $\gamma_{\text{ap}}^{[2]}$ in (47) cannot be simultaneously maximized. The optimal ζ, which minimizes the outage probability in (40), can be approximately obtained as

$$\zeta_{\text{opt}} \approx \begin{cases} \zeta_{\text{ap}}^{[1]}, & \gamma_{\text{ap}}^{[1]} > \gamma_{\text{ap}}^{[2]} \\ \zeta_{\text{ap}}^{[2]}, & \gamma_{\text{ap}}^{[1]} \leq \gamma_{\text{ap}}^{[2]}. \end{cases} \tag{49}$$

In Subsection V-A.1, we assume that $\{\alpha_{\text{SR},u,l}\}_{l=0}^{L-1}$, $\{\alpha_{\text{SR},w,l}\}_{l=0}^{L-1}$, $\{\alpha_{\text{RD},u,l}\}_{l=0}^{L-1}$, and $\{\alpha_{\text{RD},w,l}\}_{l=0}^{L-1}$ are known at the source, relay, and destination. Thus, ζ_{opt} in (49) can be readily calculated there.

Next, we determine the optimal power allocation for the two-way DTF case. For analytical tractability, we presume that the relay detects the data bits $b^{[1]}$ and $b^{[2]}$ correctly. Under this assumption, we denote $\gamma_{\text{RD}}^{[1]}$ in (42b) and $\gamma_{\text{RS}}^{[2]}$ in (43b) as $\gamma_{\text{ideal,RD}}^{[1]} = \varrho_{\text{R}}^{[1]}\mathcal{E}'_w$ and $\gamma_{\text{ideal,RS}}^{[2]} = \varrho_{\text{R}}^{[2]}\mathcal{E}_u$, respectively. Let $\zeta_{\text{ideal}}^{[1]}$ be the optimal ζ, which maximizes $\texttt{min}(\gamma_{\text{SR}}^{[1]}, \gamma_{\text{ideal,RD}}^{[1]})$. This optimal value can be found by equating $\gamma_{\text{SR}}^{[1]}$ in (42a) and $\gamma_{\text{ideal,RD}}^{[1]}$, yielding

$$\zeta_{\text{ideal}}^{[1]} = \frac{\sqrt{D_1^2 + 4\,\mathcal{E}'_w\,D_2} - D_1}{2D_2} \tag{50}$$

where $D_1 = \mathcal{E}_u + \mathcal{E}'_w - D_2$ and $D_2 = \frac{\varrho_{\text{tot}}\,\mathcal{E}'_w\mathcal{I}^2}{\mathcal{E}_u}$. Note that $D_2 > 0$ and $D_1^2 + 4\,\mathcal{E}'_w\,D_2 < (\mathcal{E}_u + \mathcal{E}'_w + D_2)^2$. Then, it is easily checked that $\zeta_{\text{ideal}}^{[1]}$ in (50) is always in the interval $(0,1)$. Likewise, the optimal ζ, which maximizes $\texttt{min}(\gamma_{\text{DR}}^{[2]}, \gamma_{\text{ideal,RS}}^{[2]})$, is given by

$$\zeta_{\text{ideal}}^{[2]} = \frac{\sqrt{D_1'^2 + 4\,\mathcal{E}_u\,D'_2} - D'_1}{2D'_2} \tag{51}$$

where $D'_1 = \mathcal{E}_u + \mathcal{E}'_w - D'_2$ and $D'_2 = \frac{\varrho_{\text{tot}}\,\mathcal{E}_u\mathcal{I}'^2}{\mathcal{E}'_w}$. It is obvious that $\texttt{min}(\gamma_{\text{SR}}^{[1]}, \gamma_{\text{ideal,RD}}^{[1]})$ and $\texttt{min}(\gamma_{\text{DR}}^{[2]}, \gamma_{\text{ideal,RS}}^{[2]})$ cannot be maximized at the same time. The optimal ζ, which minimizes the outage probability in (44), can be approximately obtained as

$$\zeta_{\text{opt}} \approx \begin{cases} \zeta_{\text{ideal}}^{[1]}, & \texttt{min}(\gamma_{\text{SR}}^{[1]}, \gamma_{\text{ideal,RD}}^{[1]}) > \texttt{min}(\gamma_{\text{DR}}^{[2]}, \gamma_{\text{ideal,RS}}^{[2]}) \\ \zeta_{\text{ideal}}^{[2]}, & \texttt{min}(\gamma_{\text{SR}}^{[1]}, \gamma_{\text{ideal,RD}}^{[1]}) \leq \texttt{min}(\gamma_{\text{DR}}^{[2]}, \gamma_{\text{ideal,RS}}^{[2]}). \end{cases} \tag{52}$$

Recall that the relay knows $\{\alpha_{\text{SR},u,l}\}_{l=0}^{L-1}$, $\{\alpha_{\text{SR},w,l}\}_{l=0}^{L-1}$, $\{\alpha_{\text{RD},u,l}\}_{l=0}^{L-1}$, and $\{\alpha_{\text{RD},w,l}\}_{l=0}^{L-1}$, while the source and destination know $\{\alpha_{\text{SR},u,l}\}_{l=0}^{L-1}$ and $\{\alpha_{\text{RD},w,l}\}_{l=0}^{L-1}$ but not $\{\alpha_{\text{SR},w,l}\}_{l=0}^{L-1}$ and $\{\alpha_{\text{RD},u,l}\}_{l=0}^{L-1}$. Therefore, the relay computes ζ_{opt} in (52), and transmits it to the source and destination through noiseless feedback links.

B. Two-Way UWB Relay Systems Using the Best Single-Antenna Relay

The system model is shown in Fig. 2(b), where the channels are assumed to be reciprocal. For these systems, we follow the assumption of partial channel knowledge at the relay in Section IV.

1) Amplify-and-Forward Relaying: Let $q^\bullet$ be the index of the best relay for this relaying scheme. The description of the data transmissions in the first and second phases can be done as in the special case (i.e., $u = w$) of the AF scheme in Subsection V-A.1, except that the antenna index u $(= w)$ is dropped, and the subscript R is replaced by the index $q^\bullet$. The best relay can be represented by its index:

$$q^\bullet = \texttt{arg}\max_{q\in\{1,2,\ldots,Q\}}\left[\texttt{max}(\gamma_q^{[1]}, \gamma_q^{[2]})\right] \tag{53}$$

where

$$\gamma_q^{[1]} = \frac{\varrho_{\text{S}}\,\mathcal{E}_q\,\varrho_q^{[1]}\,\mathcal{E}'_q + \mathcal{S}_q}{\varrho_{\text{S}}\,\mathcal{E}_q + \varrho_q^{[1]}\,\mathcal{E}'_q + 1 + \mathcal{N}_q} \tag{54}$$

with $\mathcal{S}_q = \varrho_{\text{S}}\,\varrho_q^{[2]}\left(\frac{\varrho_{\text{S}}\mathcal{E}_q^2+\varrho_{\text{D}}\mathcal{I}_q^{\,2}+\mathcal{E}_q}{\varrho_{\text{D}}\mathcal{E}_q'^2+\varrho_{\text{S}}\mathcal{I}_q^{\,2}+\mathcal{E}'_q}\right)\left(\frac{\mathcal{I}_q}{\mathcal{E}_q}\right)^2$, $\mathcal{N}_q = \frac{\varrho_{\text{D}}}{\mathcal{E}_q}\mathcal{I}_q^{\,2} + \varrho_q^{[2]}\mathcal{E}'_q\left(\frac{\varrho_{\text{S}}\mathcal{E}_q^2+\varrho_{\text{D}}\mathcal{I}_q^{\,2}+\mathcal{E}_q}{\varrho_{\text{D}}\mathcal{E}_q'^2+\varrho_{\text{S}}\mathcal{I}_q^{\,2}+\mathcal{E}'_q}\right)\left(\frac{\mathcal{I}_q}{\mathcal{E}_q}\right)^2$, $\mathcal{I}_q = \sum_{l=0}^{L-1}\alpha_{\text{S}q,l}\alpha_{\text{D}q,l}$, $\varrho_q^{[1]} = \frac{E_{b,q}^{[1]}}{N_0/2}$, and $\varrho_q^{[2]} = \frac{E_{b,q}^{[2]}}{N_0/2}$, and

$$\gamma_q^{[2]} = \frac{\varrho_q^{[2]}\,\mathcal{E}_q\,\varrho_{\text{D}}\,\mathcal{E}'_q + \mathcal{S}'_q}{\varrho_{\text{q}}^{[2]}\,\mathcal{E}_q + \varrho_{\text{D}}\,\mathcal{E}'_q + 1 + \mathcal{N}'_q} \tag{55}$$

with $\mathcal{S}'_q = \varrho_q^{[1]}\varrho_{\text{D}}\left(\frac{\varrho_{\text{D}}\mathcal{E}_q'^2+\varrho_{\text{S}}\mathcal{I}_q^{\,2}+\mathcal{E}'_q}{\varrho_{\text{S}}\mathcal{E}_q^2+\varrho_{\text{D}}\mathcal{I}_q^{\,2}+\mathcal{E}_q}\right)\left(\frac{\mathcal{I}_q}{\mathcal{E}'_q}\right)^2$ and $\mathcal{N}'_q = \frac{\varrho_{\text{S}}}{\mathcal{E}'_q}\mathcal{I}_q^{\,2} + \varrho_q^{[1]}\mathcal{E}_q\left(\frac{\varrho_{\text{D}}\mathcal{E}_q'^2+\varrho_{\text{S}}\mathcal{I}_q^{\,2}+\mathcal{E}'_q}{\varrho_{\text{S}}\mathcal{E}_q^2+\varrho_{\text{D}}\mathcal{I}_q^{\,2}+\mathcal{E}_q}\right)\left(\frac{\mathcal{I}_q}{\mathcal{E}'_q}\right)^2$. The corresponding outage probability is given by $P_{\text{out}} = \Pr\Big[\texttt{max}(\gamma_{q^\bullet}^{[1]}, \gamma_{q^\bullet}^{[2]}) \leq \gamma_{\text{th}}\Big]$, which has no closed-form expression and is obtained by means of simulations.

2) Detect-and-Forward Relaying: Let q^* be the index of the best relay for the two-way DTF scheme. The description of the data transmissions in the first and second phases can be done as in the special case (i.e., $u = w$) of the DTF scheme in Subsection V-A.2, except that the antenna index u ($= w$) is dropped, and the subscript R is replaced by the index q^*. The best relay can be represented by its index:

$$q^* = \arg \max_{q\in\{1,2,\ldots,Q\}} \left[\max\left(\min(\gamma_{\mathrm{S}q}^{[1]}, \gamma_{q\mathrm{D}}^{[1]}), \min(\gamma_{\mathrm{D}q}^{[2]}, \gamma_{q\mathrm{S}}^{[2]})\right)\right] \tag{56}$$

where

$$\gamma_{\mathrm{S}q}^{[1]} = \frac{\varrho_{\mathrm{S}}\,\mathcal{E}_q}{1+\frac{\varrho_{\mathrm{D}}\mathcal{I}_q^2}{\mathcal{E}_q}}, \tag{57a}$$

$$\gamma_{q\mathrm{D}}^{[1]} = \begin{cases} \varrho_q^{[1]}\mathcal{E}'_q\,, & \hat{b}_q^{[1]} = b^{[1]} \\ \dfrac{\varrho_q^{[1]}\mathcal{E}'_q}{1+\frac{4\varrho_q^{[2]}\mathcal{I}_q^2}{\mathcal{E}_q}}\,, & \hat{b}_q^{[1]} \neq b^{[1]}, \end{cases} \tag{57b}$$

and

$$\gamma_{\mathrm{D}q}^{[2]} = \frac{\varrho_{\mathrm{D}}\,\mathcal{E}'_q}{1+\frac{\varrho_{\mathrm{S}}\mathcal{I}_q^2}{\mathcal{E}'_q}}, \tag{58a}$$

$$\gamma_{q\mathrm{S}}^{[2]} = \begin{cases} \varrho_q^{[2]}\mathcal{E}_q\,, & \hat{b}_q^{[2]} = b^{[2]} \\ \dfrac{\varrho_q^{[2]}\mathcal{E}_q}{1+\frac{4\varrho_q^{[1]}\mathcal{I}_q^2}{\mathcal{E}'_q}}\,, & \hat{b}_q^{[2]} \neq b^{[2]}. \end{cases} \tag{58b}$$

The outage probability for this relaying scheme is given by $P_{\text{out}} = \Pr\left[\max\left(\min(\gamma_{\mathrm{S}q^*}^{[1]}, \gamma_{q^*\mathrm{D}}^{[1]}), \min(\gamma_{\mathrm{D}q^*}^{[2]}, \gamma_{q^*\mathrm{S}}^{[2]})\right) \leq \gamma_{\text{th}}\right]$, which is computed via simulations.

3) Optimal Power Allocation: The above relay selection can be combined with the optimal power allocation between the source and relay, as in Subsection IV-C. Let us first consider the two-way AF case. Following the same procedure as in Subsection V-A.3, the high-SNR approximation of $\gamma_q^{[1]}$ in (54) is obtained as $\gamma_{\text{ap},q}^{[1]} = \frac{P_{3,q}(1-\zeta)\zeta}{P_{2,q}\zeta+P_{1,q}}$, and the optimal ζ maximizing $\gamma_{\text{ap},q}^{[1]}$ is

$$\zeta_{\text{ap},q}^{[1]} = \begin{cases} \dfrac{\sqrt{P_{1,q}\left(P_{1,q}+P_{2,q}\right)} - P_{1,q}}{P_{2,q}}, & P_{2,q} \neq 0 \\ 0.5\,, & P_{2,q} = 0 \end{cases} \tag{59}$$

where $P_{1,q} = \varrho_{\text{tot}}\,\mathcal{E}'_q\left[1+\left(\frac{\mathcal{E}_q^2+\mathcal{I}_q^2}{\mathcal{E}_q'^2+\mathcal{I}_q^2}\right)\left(\frac{\mathcal{I}_q}{\mathcal{E}_q}\right)^2\right]+1$, $P_{2,q} = \varrho_{\text{tot}}\left[\mathcal{E}_q + \frac{\mathcal{I}_q^2}{\mathcal{E}_q} - \mathcal{E}'_q - \mathcal{E}'_q\left(\frac{\mathcal{E}_q^2+\mathcal{I}_q^2}{\mathcal{E}_q'^2+\mathcal{I}_q^2}\right)\left(\frac{\mathcal{I}_q}{\mathcal{E}_q}\right)^2\right]$, and $P_{3,q} = \varrho_{\text{tot}}^2\left[\mathcal{E}_q\,\mathcal{E}'_q + \left(\frac{\mathcal{E}_q^2+\mathcal{I}_q^2}{\mathcal{E}_q'^2+\mathcal{I}_q^2}\right)\left(\frac{\mathcal{I}_q^2}{\mathcal{E}_q}\right)^2\right]$. Since $P_{1,q}+P_{2,q} > 1$, it can be verified that $\zeta_{\text{ap},q}^{[1]}$ in (59) is always in the interval $(0,1)$. Similarly, the high-SNR approximation of $\gamma_q^{[2]}$ in (55) is given by $\gamma_{\text{ap},q}^{[2]} = \frac{P'_{3,q}(1-\zeta)\zeta}{P'_{2,q}\zeta+P'_{1,q}}$, and the optimal ζ maximizing $\gamma_{\text{ap},q}^{[2]}$ is

$$\zeta_{\text{ap},q}^{[2]} = \begin{cases} \dfrac{\sqrt{P'_{1,q}\;\;P'_{1,q}+P'_{2,q}\right)} - P'_{1,q}}{P'_{2,q}}, & P'_{2,q} \neq 0 \\ 0.5\,, & P'_{2,q} = 0 \end{cases} \tag{60}$$

where $P'_{1,q} = \varrho_{\text{tot}}\,\mathcal{E}_q\left[1+\left(\frac{\mathcal{E}_q'^2+\mathcal{I}_q^2}{\mathcal{E}_q^2+\mathcal{I}_q^2}\right)\left(\frac{\mathcal{I}_q}{\mathcal{E}'_q}\right)^2\right]+1$, $P'_{2,q} = \varrho_{\text{tot}}\left[\mathcal{E}'_q + \frac{\mathcal{I}_q^2}{\mathcal{E}'_q} - \mathcal{E}_q - \mathcal{E}_q\left(\frac{\mathcal{E}_q'^2+\mathcal{I}_q^2}{\mathcal{E}_q^2+\mathcal{I}_q^2}\right)\left(\frac{\mathcal{I}_q}{\mathcal{E}'_q}\right)^2\right]$, and $P'_{3,q} = \varrho_{\text{tot}}^2\left[\mathcal{E}_q\,\mathcal{E}'_q + \left(\frac{\mathcal{E}_q'^2+\mathcal{I}_q^2}{\mathcal{E}_q^2+\mathcal{I}_q^2}\right)\left(\frac{\mathcal{I}_q^2}{\mathcal{E}'_q}\right)^2\right]$. It is straightforward to show that the optimal ζ maximizing the term $\min(\gamma_q^{[1]}, \gamma_q^{[2]})$ in (53) is approximately

$$\zeta_{\text{opt},q} \approx \begin{cases} \zeta_{\text{ap},q}^{[1]}\,, & \gamma_{\text{ap},q}^{[1]} > \gamma_{\text{ap},q}^{[2]} \\ \zeta_{\text{ap},q}^{[2]}\,, & \gamma_{\text{ap},q}^{[1]} \leq \gamma_{\text{ap},q}^{[2]}. \end{cases} \tag{61}$$

At the q-th relay, $\min(\gamma_q^{[1]}, \gamma_q^{[2]})$ is then computed using (54), (55), (59)-(61). Only the relay with the largest value of this maximum is chosen as the active relay.[12] For the same reason as in the AF scheme in Subsection V-A.3, the optimal ζ in (61) corresponding to the active relay can be calculated at the source and destination.

Next, we introduce the relay selection with optimal power allocation for the two-way DTF scheme. For analytical tractability, we presume that any of the available relays detects the data bits $b^{[1]}$ and $b^{[2]}$ correctly. Under this assumption, we denote $\gamma_{q\mathrm{D}}^{[1]}$ in (57b) and $\gamma_{q\mathrm{S}}^{[2]}$ in (58b) as $\gamma_{\text{ideal},q\mathrm{D}}^{[1]} = \varrho_q^{[1]}\mathcal{E}'_q$ and $\gamma_{\text{ideal},q\mathrm{S}}^{[2]} = \varrho_q^{[2]}\mathcal{E}_q$, respectively. Following the same procedure as in Subsection V-A.3, the optimal ζ, which maximizes $\min(\gamma_{\mathrm{S}q}^{[1]}, \gamma_{\text{ideal},q\mathrm{D}}^{[1]})$, is obtained as

$$\zeta_{\text{ideal},q}^{[1]} = \frac{\sqrt{W_{1,q}^2 + 4\,\mathcal{E}'_q\,W_{2,q}} - W_{1,q}}{2W_{2,q}} \tag{62}$$

where $W_{1,q} = \mathcal{E}_q + \mathcal{E}'_q - W_{2,q}$ and $W_{2,q} = \frac{\varrho_{\text{tot}}\,\mathcal{E}'_q\mathcal{I}_q^2}{\mathcal{E}_q}$. Note that $W_{2,q} > 0$ and $W_{1,q}^2 + 4\,\mathcal{E}'_q\,W_{2,q} < (\mathcal{E}_q + \mathcal{E}'_q + W_{2,q})^2$. Thus, it is easily checked that $\zeta_{\text{ideal},q}^{[1]}$ in (62) is always in the interval $(0,1)$. Similarly, the optimal ζ, which maximizes $\min(\gamma_{\mathrm{D}q}^{[2]}, \gamma_{\text{ideal},q\mathrm{S}}^{[2]})$, is given by

$$\zeta_{\text{ideal},q}^{[2]} = \frac{\sqrt{W_{1,q}'^2 + 4\,\mathcal{E}_q\,W'_{2,q}} - W'_{1,q}}{2W'_{2,q}} \tag{63}$$

where $W'_{1,q} = \mathcal{E}_q + \mathcal{E}'_q - W'_{2,q}$ and $W'_{2,q} = \frac{\varrho_{\text{tot}}\,\mathcal{E}_q\mathcal{I}_q^2}{\mathcal{E}'_q}$. It is straightforward to show that the optimal ζ maximizing the term $\max\left(\min(\gamma_{\mathrm{S}q}^{[1]}, \gamma_{q\mathrm{D}}^{[1]}), \min(\gamma_{\mathrm{D}q}^{[2]}, \gamma_{q\mathrm{S}}^{[2]})\right)$ in (56) is approximately

$$\zeta_{\text{opt},q} \approx \begin{cases} \zeta_{\text{ideal},q}^{[1]}, & \min(\gamma_{\mathrm{S}q}^{[1]}, \gamma_{\text{ideal},q\mathrm{D}}^{[1]}) > \min(\gamma_{\mathrm{D}q}^{[2]}, \gamma_{\text{ideal},q\mathrm{S}}^{[2]}) \\ \zeta_{\text{ideal},q}^{[2]}, & \min(\gamma_{\mathrm{S}q}^{[1]}, \gamma_{\text{ideal},q\mathrm{D}}^{[1]}) \leq \min(\gamma_{\mathrm{D}q}^{[2]}, \gamma_{\text{ideal},q\mathrm{S}}^{[2]}). \end{cases} \tag{64}$$

At the q-th relay, $\max\left(\min(\gamma_{\mathrm{S}q}^{[1]}, \gamma_{q\mathrm{D}}^{[1]}), \min(\gamma_{\mathrm{D}q}^{[2]}, \gamma_{q\mathrm{S}}^{[2]})\right)$ is therefore calculated using (57), (58), (62)-(64). Only the relay with the largest value of this maximum is chosen as the active relay. For the same reason as in the DTF scheme in Subsection V-A.3, this active relay sends its optimal ζ in (64) to the source and destination via error-free feedback channels.

[12] Such relay selection can be practically realized using the protocol suggested in [49] with certain parameter modification.

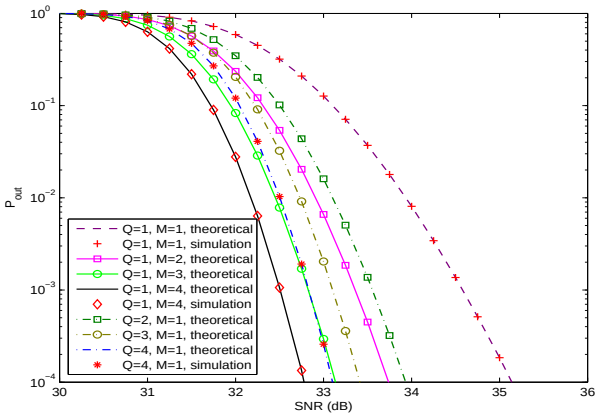

Figure 3. Outage probabilities of the one-way AF systems in symmetric channels (d m, ζ .5).

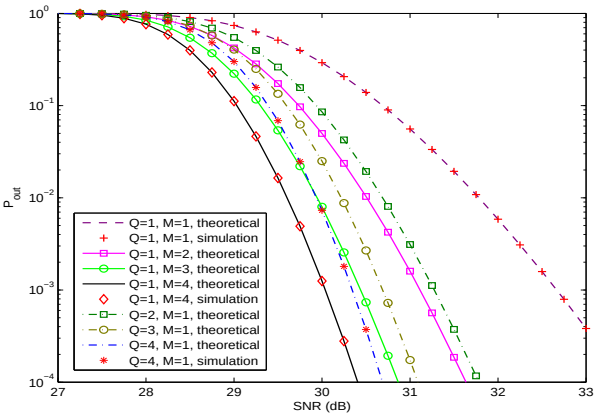

Figure 4. Outage probabilities of the one-way DTF systems in symmetric channels (d m, ζ .5).

VI. Numerical Results

In this section, some numerical examples of the results derived in this paper are presented. In Figs. 1(a) and 2(a), it is assumed that the source and destination are separated by a distance of 8 meters (m), and the multiple-antenna relay is located in a line between them. Let d denote the distance from the source to the relay (in m), and hence the distance from the relay to the destination is $8-d$ m. The total multipath gains G_{SR} and G_{RD} are calculated according to the UWB path loss model described in [31, eq. (1)]. Recall that the antenna index j is dropped for notational simplicity. In generating the UWB energy-normalized channel coefficients $\{\varphi_{\text{SR},l}\}_{l=0}^{L-1}$ and $\{\varphi_{\text{RD},l}\}_{l=0}^{L-1}$, we assume that $T_g = 2$ ns, $L_t = 50$, $m_{\text{SR}} = m_{\text{RD}} = 2$, $\Omega_{\text{SR},0} = \Omega_{\text{RD},0} = 0.054$, and $\varpi_{\text{SR}} = \varpi_{\text{RD}} = 0.95$ [39]. These parameter settings are also used in Figs. 1(b) and 2(b), where the subscript R is replaced by the relay index q since the Q single-antenna relays are considered in lieu of the multiple-antenna relay. To simplify simulations, we assume that $N_f = 1$. Unless stated otherwise, the number of Rake/pre-Rake fingers (L) is chosen to be 10, which is a good compromise between performance and complexity [47], [53], and the SNR threshold (γ_{th}) is set to be 10 dB.

A. One-Way Relay Systems

Fig. 3 shows the theoretical outage probabilities of the one-way AF systems using the multiple-antenna relay with the antenna selection (i.e, $Q = 1$ and $M > 1$, and computed with (14)-(16)), and those using the best relay among the Q available single-antenna relays (i.e., $Q > 1$ and $M = 1$, and computed with (25) and (26)). For comparison, the simulated outage curves are also plotted. The abscissa indicates the total transmitted SNR (ϱ_{tot}). In this figure, we consider the symmetric channel case where the relays are located halfway between the corresponding source and destination, i.e., $d = 4$ m, and assume equal power allocation between the source and the (best) relay, i.e., $\zeta = 0.5$ in (21). The theoretical and simulated outage curves of the baseline AF system (i.e, $Q = 1$ and $M = 1$) are also included in the figure. We can see that the theoretical results perfectly match their simulation counterparts, which verifies the outage probability formulae in (14)-(16) and in (25) and (26). The outage performance of the AF systems using the multiple-antenna relay with the antenna selection improves as M increases. Furthermore, the outage probabilities of the AF systems using the single-antenna relay selection decrease with the increase of Q. When the product of Q and M is fixed, i.e., when $QM = 2, 3$, and 4, respectively, the AF system using the multiple-antenna relay with the antenna selection performs better than that using the single-antenna relay selection. This also holds true for the case of optimal power allocation, as will be seen in Fig. 5. Basically, this is due to the fact that the multiple-antenna relay has an *additional degree of freedom in choosing the best transmit and receive antennas*. The performance gap between the two systems increases with QM. Similar performance trends can be observed in the one-way DTF systems as illustrated in Fig. 4 (where the theoretical outage probabilities are computed with (19) for $Q = 1$ and $M > 1$, and computed with (28) and (29) for $Q > 1$ and $M = 1$). Comparing Fig. 4 with Fig. 3, one can see that the DTF systems using the multiple-antenna relay with the antenna selection are superior to their AF counterparts. The superiority of the former systems is because of the additional signal processing, i.e., the hard decision, at the relay. For the same reason, the DTF systems using the single-antenna relay selection achieve a lower outage probability compared to their AF counterparts.

Fig. 5 depicts the outage performance comparisons between the aforementioned AF systems with equal power allocation ($\zeta = 0.5$) and those with optimal power allocation (ζ_{opt} in (22) for $Q = 1$ and $M = 4$, and $\zeta_{\text{opt},q}$ in (30) for $Q = 4$ and $M = 1$), when $\varrho_{\text{tot}} = 33$ dB. The outage results for the latter systems can only be obtained through simulations, as the optimal power allocation requires partial knowledge of the corresponding

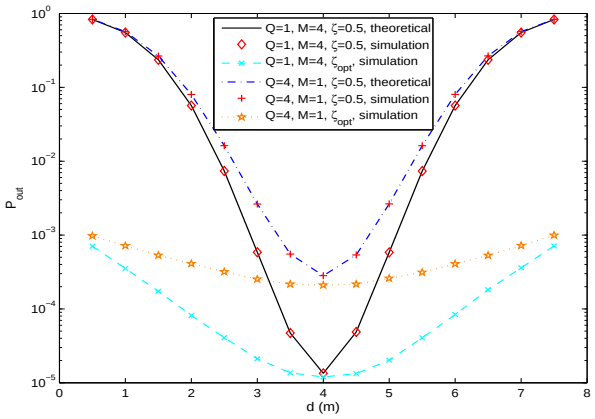

Figure 5. Impact of power optimization on the performance of the one-way AF systems.

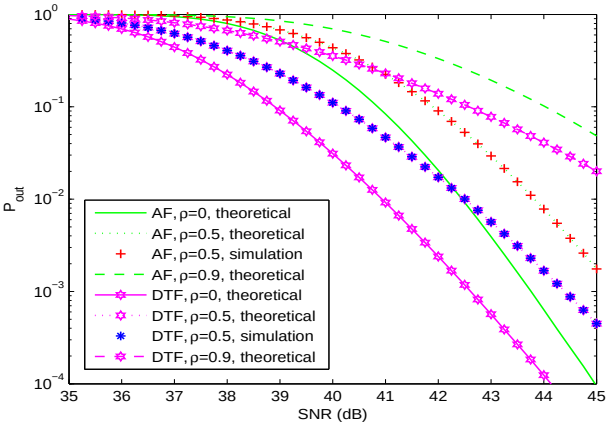

Figure 7. Effect of the spatial correlation coefficient ρ on the performance of the one-way AF and DTF systems (d m, ζ .5, Q 1, M , L 1).

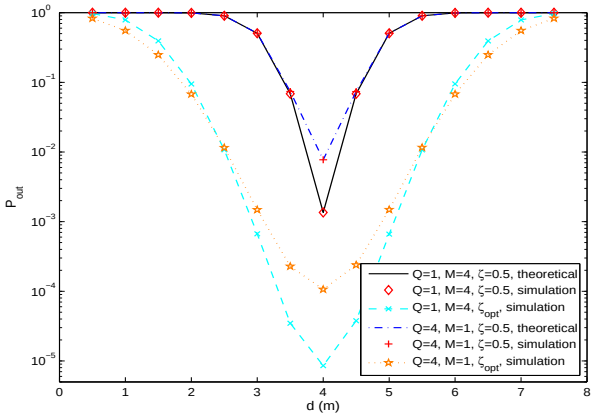

Figure 6. Impact of power optimization on the performance of the one-way DTF systems.

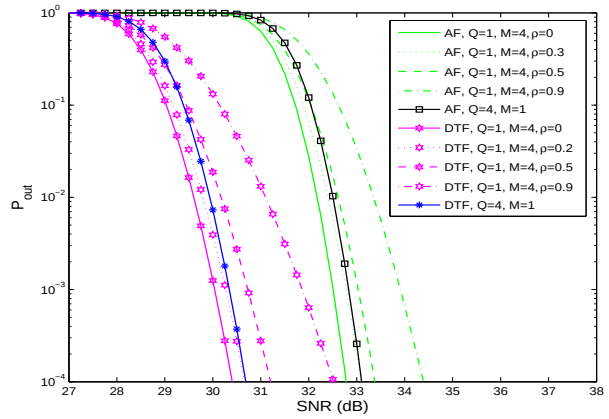

Figure 8. Effect of the spatial correlation coefficient ρ on the performance of the one-way AF and DTF systems (d m, ζ .5, L 1).

instantaneous CSI [see (22) and (30)]. From Fig. 5, it is clear that the optimal power allocation for both the AF system with $Q = 1$ and $M = 4$, and the one with $Q = 4$ and $M = 1$ enhances the system performance, especially when the relay is very close to the source (d approaches 0 m) or the destination (d approaches 8 m). However, at the halfway point between the source and destination ($d = 4$ m), the gains of optimizing the power allocation are minimal. As a result, when the relay is located in the vicinity of this point, using equal power between the source and relay is a good strategy. In Fig. 6, we compare the outage probabilities of the DTF systems with equal power allocation ($\zeta = 0.5$) and those with optimal power allocation (ζ_{opt} in (23) for $Q = 1$ and $M = 4$, and $\zeta_{\text{opt},q}$ in (31) for $Q = 4$ and $M = 1$), when $\varrho_{\text{tot}} = 30$ dB. In contrast to the results in Fig. 5, a substantial improvement in the outage performance of the DTF systems by optimizing the power allocation is observed when the relay is near the midpoint between the source and destination (d is between 3 m and 5 m). Both figures show that in all the considered systems, the best position for the relay is the halfway point between the source and destination.

The spatial correlation between the antennas at the multiple-antenna relay is not taken into account so far. From a practical point of view, it is important to investigate how such correlation affects the corresponding system performance. In Appendix A, the CDFs and PDFs of $\mathcal{E}_u$ and $\mathcal{E}'_w$ for the spatial correlation case with $L = 1$ are provided. Based on these functions, the theoretical outage probabilities of the AF and DTF systems using the multiple-antenna relay with the antenna selection are obtained by numerically computing the third line of (14) and the fourth line of (19), respectively. Fig. 7 illustrates the effect of the spatial correlation, represented by ρ (see Appendix A), on these outage probabilities with $M = 4$ and $L = 1$, assuming $\zeta = 0.5$ and $d = 4$ m. The simulated outage curves are also included to compare with the theoretical outage curves. It can be seen that the outage performance degrades as the spatial correlation increases. As mentioned in Appendix A, there are no closed-form expressions for the CDFs and PDFs of $\mathcal{E}_u$ and

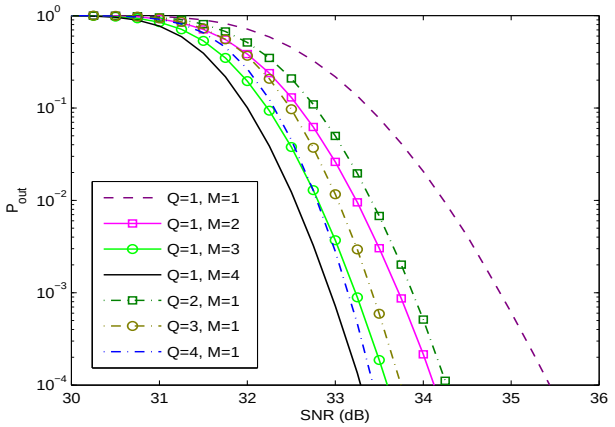

Figure 9. Outage probabilities of the two-way AF systems in symmetric channels (d m, ζ .5).

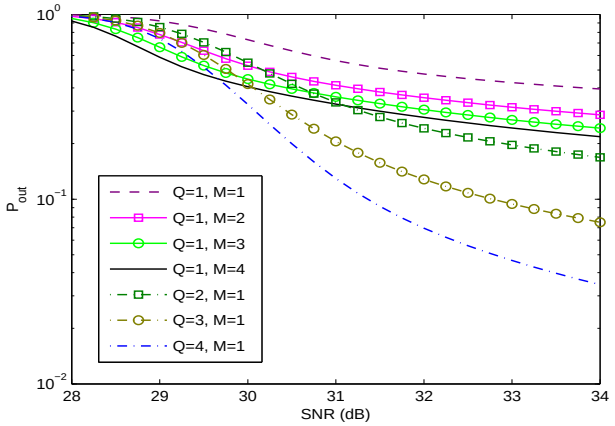

Figure 10. Outage probabilities of the two-way DTF systems in symmetric channels (d m, ζ .5).

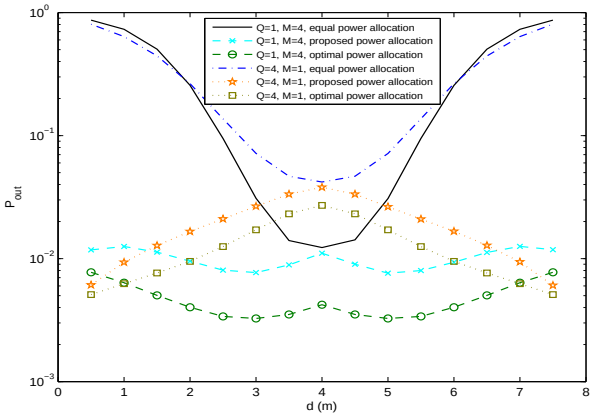

Figure 11. Impact of power optimization on the performance of the two-way AF systems.

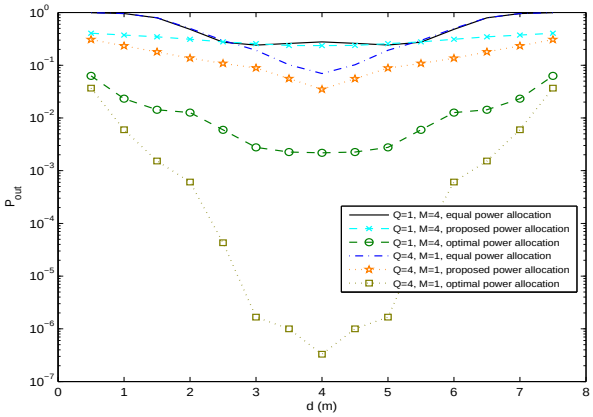

Figure 12. Impact of power optimization on the performance of the two-way DTF systems.

$\mathcal{E}'_w$ in the spatial correlation case with $L > 1$. To obtain the outage results for this case, we apply the simulation approach presented in [54, Subsection 2.4] (see the given reference for details). The simulation results for $M = 4$ and $L = 10$ are shown in Fig. 8. For comparison, the simulated outage curves of the systems using the best relay with $Q = 4$ and $L = 10$ are also included. We can observe that, in the outage probability range of interest, the AF and DTF systems using the multiple-antenna relay with the antenna selection are superior to those using the single-antenna relay selection when $\rho \leq 0.3$ and $\rho \leq 0.2$, respectively. The spatial correlation in UWB channels depends primarily on antenna spacing [24]. Thus, deploying the multiple-antenna relay with the antenna selection is a better option although the antenna spacing at the relay needs to be carefully designed.

B. Two-Way Relay Systems

In Figs. 9-12, all the results are obtained via simulations. Fig. 9 shows the outage probabilities of the two-way AF systems using the multiple-antenna relay with the antenna selection (computed with (40)) and those using the single-antenna relay selection (computed with $\Pr\big[\max(\gamma_{q^\bullet}^{[1]}, \gamma_{q^\bullet}^{[2]}) \leq \gamma_{\text{th}}\big]$). In this figure, equal power allocation (i.e., $\varrho_{\text{S}} = \varrho_{\text{D}} = \varrho_{\text{R}}^{[1]}$ (or $\varrho_q^{[1]}$) $= \varrho_{\text{R}}^{[2]}$ (or $\varrho_q^{[2]}$) $= 0.5\,\varrho_{\text{tot}}$) and $d = 4$ m are assumed, and the outage curve of the baseline two-way AF system (i.e, $Q = 1$ and $M = 1$) is also plotted. Similar to the one-way AF cases, increasing the numbers of antennas and relays improves, respectively, the outage performance of the two-way AF systems using the multiple-antenna relay with the antenna selection and those using the single-antenna relay selection. Furthermore, with the same value of QM, the former systems outperform the latter ones.

Fig. 10 plots the outage probabilities of the two-way DTF systems (computed with (44) for $Q = 1$ and $M > 1$, and computed with $\Pr\big[\max \min(\gamma_{\text{S}q^*}^{[1]}, \gamma_{q^*\text{D}}^{[1]}), \min(\gamma_{\text{D}q^*}^{[2]}, \gamma_{q^*\text{S}}^{[2]})\big) \leq \gamma_{\text{th}}\big]$ for $Q > 1$ and $M = 1$) under the same parameter settings as in Fig. 9. Somewhat surprisingly, in the high SNR regime, the two-way DTF system with $Q = 1$ and $M = 4$ performs even worse than that with $Q = 2$ and $M = 1$. This is in contrast to the results for the one-way DTF systems in Fig. 4. Note that there exist outage floors

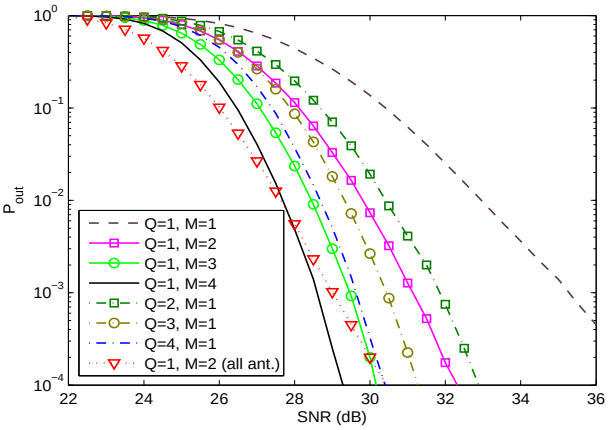

Figure 13. Outage probabilities of the one-way AF systems in an IEEE 802.15.3a UWB channel (CM1, d m, ζ .5).

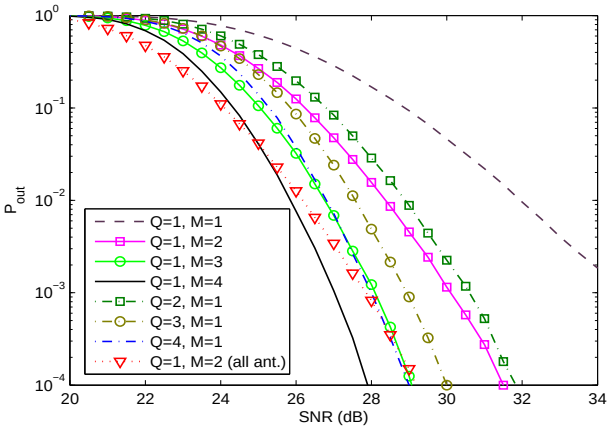

Figure 14. Outage probabilities of the one-way DTF systems in an IEEE 802.15.3a UWB channel (CM1, d m, ζ .5).

in the two-way DTF systems, which is mainly due to the erroneous data bit detection at the relay. Comparing Figs. 9 and 10, we observe that the two-way AF systems have lower outage probabilities than their two-way DTF counterparts at high SNRs, say more than 32 dB. From Figs. 3, 4, 9, and 10, it is evident that the two-way relaying schemes are inferior to the one-way relaying schemes in terms of their outage probabilities.

Fig. 11 compares the outage performance of the two-way AF systems using the equal power allocation strategy, and the power allocation strategies proposed in Subsections V-A.3 and V-B.3 (i.e., $\varrho_{\rm S} = \varrho_{\rm D} = \zeta\,\varrho_{\rm tot}$ and $\varrho_{\rm R}^{[1]}$ (or $\varrho_q^{[1]}$) $= \varrho_{\rm R}^{[2]}$ (or $\varrho_q^{[2]}$) $= (1-\zeta)\,\varrho_{\rm tot}$ where ζ is equal to $\zeta_{\rm opt}$ in (49) for $Q = 1$ and $M = 4$, and ζ is equal to $\zeta_{{\rm opt},q}$ in (61) for $Q = 4$ and $M = 1$), when $\varrho_{\rm tot} = 32.5$ dB. As a reference, we also plot the outage curves corresponding to the case where $E_{b,{\rm S}}$, $E_{b,{\rm R}}^{[1]}$ (or $E_{b,q}^{[1]}$), $E_{b,{\rm R}}^{[2]}$ (or $E_{b,q}^{[2]}$), and $E_{b,{\rm D}}$ are all optimized subject to the constraint $E_{b,{\rm S}} + E_{b,{\rm R}}^{[1]}$ (or $E_{b,{\rm S}} + E_{b,q}^{[1]}$) $= E_{b,{\rm R}}^{[2]} + E_{b,{\rm D}}$ (or $E_{b,q}^{[2]} + E_{b,{\rm D}}$) $= E_b$. Such power optimization can only be achieved by exhaustive search and, therefore, is much more time-consuming compared with our proposed power allocation strategies. The results in Fig. 11 show that the proposed strategies are beneficial, particularly when the relay is located near the source or the destination. Fig. 12 illustrates the effectiveness of our proposed power allocation strategies for the two-way DTF cases (i.e., $\zeta_{\rm opt}$ in (52) for $Q = 1$ and $M = 4$, and $\zeta_{{\rm opt},q}$ in (64) for $Q = 4$ and $M = 1$), when $\varrho_{\rm tot} = 32$ dB. Recollect that these strategies are derived based on the assumption that there are no data detection errors at the relay, but we do not make this assumption in our simulations. The outage probabilities obtained with such strategies may be worst than those obtained with the equal power allocation strategy. However, we find in our simulation trials that if this case happens, the outage performance difference is very small and can be neglected, e.g., the performance difference between the system with $Q = 1, M = 4$ using $\zeta = 0.5$ and the one using $\zeta_{\rm opt}$ when $d = 3$ m in Fig. 12.

C. System Performance in an IEEE 802.15.3a UWB Channel

While the above performance results are based on the TDL channel model suited for dense multipath environments, it is worthwhile to investigate the outage performance of the aforementioned UWB relay systems in sparse multipath channels. As discussed in Section II, a sparse channel model such as the IEEE 802.15.3a channel model is relatively complicated, which prohibits the theoretical performance analysis of those systems. Therefore, we present simulation results instead. In our simulations, we consider the symmetric channel case described previously and assume equal power allocation between the source and the (best) relay. According to the IEEE 802.15.3a channel model, the source-relay and relay-destination links (line-of-sight, 4 m) belong to channel model CM1 [35] where the sampling time is chosen to be 2 ns, and the path loss model of [55] is assumed.[13] Figs. 13 and 14 show the simulated outage probabilities of the one-way AF and one-way DTF systems, respectively, with the same SNR threshold and number of Rake fingers as before. Comparing Figs. 3 and 13 (or Figs. 4 and 14), we see that the performance benefits of the antenna selection at the multiple-antenna relay ($Q = 1$ and $M > 1$) and of the single-antenna relay selection ($Q > 1$ and $M = 1$) in the IEEE 802.15.3a channel are more pronounced than in the dense multipath channel. For instance, at BER = 10^{-3}, the one-way AF system with $Q = 1$ and $M = 4$ has a 3.3-dB SNR gain compared to that with $Q = 1$ and $M = 1$ in the former channel, but has a 2-dB SNR gain in the latter channel. However, the relative performance of the one-way AF (or one-way DTF) system with $Q = 1$ and $M > 1$, and that with $Q > 1$ and $M = 1$ remains the same for the two distinct channels. Similar trends can

[13] Notice that the path loss model for the IEEE 802.15.3a channel model is different from that for the TDL channel model. This leads to different SNR ranges of interest in the outage results for the same system but different channel models. For example, the SNR range of interest in Fig. 3 is from 22 to 36 dB, while that in Fig. 13 is from 30 to 36 dB.

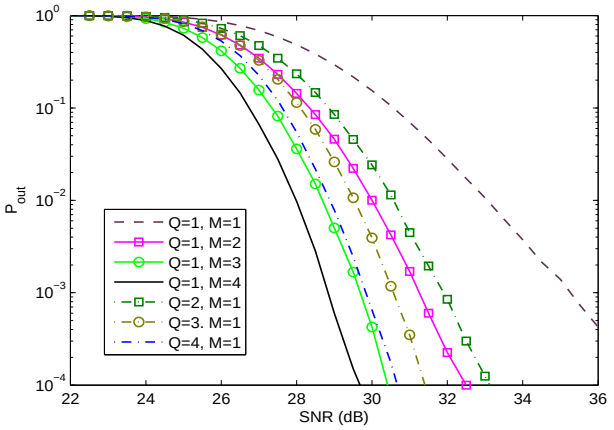

Figure 15. Outage probabilities of the two-way AF systems in an IEEE 802.15.3a UWB channel (CM1, d m, ζ .5).

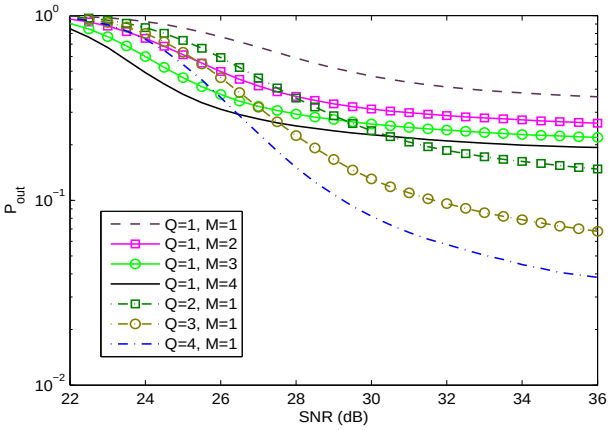

Figure 16. Outage probabilities of the two-way DTF systems in an IEEE 802.15.3a UWB channel (CM1, d m, ζ .5).

also be observed in the two-way AF (or two-way DTF) systems, as illustrated in Fig. 15 (or Fig. 16).

Note that the simulated outage curves of the one-way AF and one-way DTF systems using the two-antenna relay, where *both antennas are used*[14] for reception as well as transmission (labeled with "all ant."), are included in Figs. 13 and 14, respectively. These systems are more complex and expensive than the one-way AF and one-way DTF systems using the multiple-antenna relay with *single-antenna selection*, respectively, because 1) the complexity and cost of the radio front end scale with the number of antennas used [14], [15] and 2) the total number of Rake/pre-Rake fingers used in the former systems (i.e., 20) is twice that used in the latter systems (i.e., 10). It can be seen from both figures that, in the high SNR regime, the two-antenna relay systems (without such antenna selection) yield worse performance than the four-antenna relay systems with the antenna selection, and comparable performance to the three-antenna relay systems with the antenna selection. In practice, it would thus be preferable to use only the best transmit antenna and best receive antenna in UWB multiple-antenna relay systems.

VII. Conclusion

In this paper, we have presented *one-way and two-way UWB* relay systems using a multiple-antenna relay with antenna selection, and those using single-antenna relay selection. Our focus is on AF and DTF relaying schemes for these systems. We have derived the *exact* expressions for the end-to-end SNR outage probabilities of one-way AF and one-way DTF relay systems over a UWB dense multipath channel. With the objective of minimizing these outage probabilities, the optimal power allocation strategies are developed. We also have presented the SNR expressions for the received signals in two-way AF and two-way DTF relay systems. Based on these expressions, the power allocation strategies, which approximately minimize the corresponding outage probabilities, are proposed. The numerical results have shown that for the one-way AF, one-way DTF, and two-way AF systems, using the multiple-antenna relay with the antenna selection generally offers more outage improvement than using the single-antenna relay selection. However, *this conclusion is not valid for the two-way DTF systems*. We have examined the performance gains of the aforementioned power allocation strategies over the equal power allocation strategy, and demonstrated how these gains are affected by the relative position of the relay with respect to the source and destination.

[14]For details, see, e.g., [12].

Appendix

A. CDFs and PDFs of $\mathcal{E}_u$ and $\mathcal{E}'_w$

Referring back to Section II, let us first consider the case that the channel coefficients $\{\alpha_{\mathrm{SR},j,l}\}_{j=1}^{M}$ are statistically independent and so are $\{\alpha_{\mathrm{RD},j,l}\}_{j=1}^{M}$. We refer to this case as *spatial uncorrelation case*. In order to find the CDF and PDF of $\mathcal{E}_u = \max_{j\in\{1,\ldots,M\}} \mathcal{E}_j$, we need to find the CDF and PDF of $\mathcal{E}_j = \sum_{l=0}^{L-1} \xi_{j,l}$ where $\xi_{j,l} = \alpha_{\mathrm{SR},j,l}^2$. For notational simplicity but without causing confusion, hereafter we omit the antenna index j while keeping the antenna indexes u and w. Let us define $\Phi_{\mathrm{SR},l} = G_{\mathrm{SR}}\eta_{\mathrm{SR},l} = G_{\mathrm{SR}}\Omega_{\mathrm{SR},l}/m_{\mathrm{SR}}$ and $\Phi_{\mathrm{RD},l} = G_{\mathrm{RD}}\eta_{\mathrm{RD},l} = G_{\mathrm{RD}}\Omega_{\mathrm{RD},l}/m_{\mathrm{RD}}$ for ease of exposition. Using (3), (4) and with the help of [56, eq. (7)], we obtain

$$f_{\xi_l}(x; m_{\mathrm{SR}}, \Phi_{\mathrm{SR},l}) = \frac{x^{m_{\mathrm{SR}}-1}}{\Phi_{\mathrm{SR},l}^{m_{\mathrm{SR}}}(m_{\mathrm{SR}}-1)!}\exp\left(-\frac{x}{\Phi_{\mathrm{SR},l}}\right)U(x) \tag{65}$$

and

$$\begin{aligned} F_{\xi_l}(x; m_{\mathrm{SR}}, \Phi_{\mathrm{SR},l}) &= \left[1 - \frac{\left(m_{\mathrm{SR}}, \frac{x}{\Phi_{\mathrm{SR},l}}\right)}{(m_{\mathrm{SR}}-1)!}\right]U(x) \\ &= \left[1 - e^{-\frac{x}{\Phi_{\mathrm{SR},l}}}\sum_{v=0}^{m_{\mathrm{SR}}-1}\frac{1}{v!}\left(\frac{x}{\Phi_{\mathrm{SR},l}}\right)^v\right]U(x). \end{aligned} \tag{66}$$

Applying Theorem 1 in [57], the PDF and CDF of $\mathcal{E}$ can be derived, respectively, as

$$f_{\mathcal{E}}(x)=\sum_{l=0}^{L-1}\sum_{k=1}^{m_{\text{SR}}}\Delta(l,k,m_{\text{SR}},\{\Phi_{\text{SR},\ell}\}_{\ell=0}^{L-1})\, f_{\xi_l}(x;k,\Phi_{\text{SR},l}), \tag{67}$$

$$F_{\mathcal{E}}(x)=\sum_{l=0}^{L-1}\sum_{k=1}^{m_{\text{SR}}}\Delta(l,k,m_{\text{SR}},\{\Phi_{\text{SR},\ell}\}_{\ell=0}^{L-1})\, F_{\xi_l}(x;k,\Phi_{\text{SR},l}) \tag{68}$$

where

$$\begin{aligned}\Delta(l,k,m_{\text{SR}},\{\Phi_{\text{SR},\ell}\}_{\ell=0}^{L-1})&=\frac{(-1)^{(L-1)m_{\text{SR}}}\,\Phi_{\text{SR},l}^{k}}{[(m_{\text{SR}}-1)!]^{L-1}\prod_{\ell=0}^{L-1}\Phi_{\text{SR},\ell}^{m_{\text{SR}}}}\\ &\times\sum_{i_1=k}^{m_{\text{SR}}}\sum_{i_2=k}^{i_1}\cdots\sum_{i_{L-2}=k}^{i_{L-3}}\Bigg[\frac{(2m_{\text{SR}}-i_1-1)!\,(i_{L-2}+m_{\text{SR}}-k-1)!}{(m_{\text{SR}}-i_1)!\,(i_{L-2}-k)!}\\ &\times\left(\frac{1}{\Phi_{\text{SR},l}}-\frac{1}{\Phi_{\text{SR},L-2+U(L-2-l)}}\right)^{k-i_{L-2}-m_{\text{SR}}}\\ &\times\left(\frac{1}{\Phi_{\text{SR},l}}-\frac{1}{\Phi_{\text{SR},0+U(-l)}}\right)^{i_1-2m_{\text{SR}}}\prod_{p=1}^{L-3}\frac{(m_{\text{SR}}+i_p-i_{p+1}-1)!}{(i_p-i_{p+1})!}\\ &\times\left(\frac{1}{\Phi_{\text{SR},l}}-\frac{1}{\Phi_{\text{SR},p+U(p-l)}}\right)^{i_{p+1}-i_p-m_{\text{SR}}}\Bigg].\end{aligned} \tag{69}$$

Following [57, eq. (8)], we can calculate $\Delta(l,k,m_{\text{SR}},\{\Phi_{\text{SR},\ell}\}_{\ell=0}^{L-1})$ recursively as

$$\begin{aligned}\Delta(l,m_{\text{SR}}-k,m_{\text{SR}},\{\Phi_{\text{SR},\ell}\}_{\ell=0}^{L-1})&=\frac{m_{\text{SR}}}{k}\sum_{\substack{p,\ell=0\\ \ell\neq l}}^{L-1}\frac{1}{\Phi_{\text{SR},l}^{p+1}}\\ &\times\left(\frac{1}{\Phi_{\text{SR},l}}-\frac{1}{\Phi_{\text{SR},\ell}}\right)^{-(p+1)}\Delta(l,m_{\text{SR}}-k+p+1,m_{\text{SR}},\{\Phi_{\text{SR},\ell}\}_{\ell=0}^{L-1})\end{aligned} \tag{70}$$

with $\Delta(l,k,m_{\text{SR}},\{\Phi_{\text{SR},\ell}\}_{\ell=0}^{L-1}) = \frac{1}{\prod_{\substack{\ell=0,\\ \ell\neq l}}^{L-1}\Phi_{\text{SR},\ell}^{m_{\text{SR}}}}\prod_{\substack{p=0,\\ p\neq l}}^{L-1}\left(\frac{1}{\Phi_{\text{SR},p}}-\frac{1}{\Phi_{\text{SR},l}}\right)^{-m_{\text{SR}}}$. Using (65)-(68) and [58, Ex. 8-2], and defining

$$\Xi_k=\frac{1}{(k-1)!\,\Phi_{\text{SR},l}^{k-1}}\sum_{c=k}^{m_{\text{SR}}}\Delta(l,c,m_{\text{SR}},\{\Phi_{\text{SR},\ell}\}_{\ell=0}^{L-1}), \tag{71}$$

the CDF and PDF of $\mathcal{E}_u$ can be expressed, respectively, as

$$F_{\mathcal{E}_u}(x) =\left[1+\sum_{v=1}^{M}(-1)^v\binom{M}{v}\sum_{l_1=0}^{L-1}\sum_{k_1=1}^{m_{\text{SR}}}\cdots\sum_{l_v=0}^{L-1}\sum_{k_v=1}^{m_{\text{SR}}}\prod_{p=1}^{v}\Xi_{k_p}x^{A_1}e^{-A_2x}\right]U(x), \tag{72}$$

$$\begin{aligned}f_{\mathcal{E}_u}(x)=M\sum_{l=0}^{L-1}\sum_{k=1}^{m_{\text{SR}}}\Delta(l,k,m_{\text{SR}},\{\Phi_{\text{SR},\ell}\}_{\ell=0}^{L-1})\frac{x^{k-1}}{\Phi_{\text{SR},l}^{k}(k-1)!}\\ \times\exp\left(-\frac{x}{\Phi_{\text{SR},l}}\right)\Bigg[1+\sum_{v=1}^{M-1}(-1)^v\binom{M-1}{v}\\ \times\sum_{l_1=0}^{L-1}\sum_{k_1=1}^{m_{\text{SR}}}\cdots\sum_{l_v=0}^{L-1}\sum_{k_v=1}^{m_{\text{SR}}}\prod_{p=1}^{v}\Xi_{k_p}x^{A_1}e^{-A_2x}\Bigg]U(x)\end{aligned} \tag{73}$$

where $A_1=\sum_{p=1}^{v}k_p-v$ and $A_2=\sum_{p=1}^{v}\frac{1}{\Phi_{\text{SR},l_p}}$. Similarly, the CDF and PDF of $\mathcal{E}_w'$ are obtained as (72) and (73), respectively, both with m_{SR}, $\Phi_{\text{SR},\ell}$ (and $\Phi_{\text{SR},l}$), $\{l_p\}_{p=1}^{v}$, $\{k_p\}_{p=1}^{v}$, Ξ_{k_p}, A_1, and A_2 being replaced by m_{RD}, $\Phi_{\text{RD},\ell'}$ (and $\Phi_{\text{RD},l'}$), $\{l_{p'}'\}_{p'=1}^{v'}$, $\{k_{p'}'\}_{p'=1}^{v'}$, $\Xi_{k_{p'}'}'=\frac{1}{(k_{p'}'-1)!\,\Phi_{\text{RD},l'}^{k_{p'}'-1}}\sum_{c'=k_{p'}'}^{m_{\text{RD}}}\Delta(l',c',m_{\text{RD}},\{\Phi_{\text{RD},\ell'}\}_{\ell'=0}^{L-1})$, $A_3=\sum_{p'=1}^{v'}k_{p'}'-v'$, and $A_4=\sum_{p'=1}^{v'}\frac{1}{\Phi_{\text{RD},l_{p'}'}}$, respectively.

Next, we consider the so-called *spatial correlation case* where the channel coefficients $\{\alpha_{\text{SR},j,l}\}_{j=1}^{M}$ are statistically correlated and so are $\{\alpha_{\text{RD},j,l}\}_{j=1}^{M}$. Let us define the correlation coefficient between $\xi_{j,l}$ and $\xi_{j',l}$ as $\rho_{j,j'}=\text{Cov}[\xi_{j,l},\xi_{j',l}]/\sqrt{\text{Var}[\xi_{j,l}]\text{Var}[\xi_{j',l}]}$, and the one between $\xi_{j,l}'$ and $\xi_{j',l}'$ as $\rho_{j,j'}'=\text{Cov}[\xi_{j,l}',\xi_{j',l}']/\sqrt{\text{Var}[\xi_{j,l}']\text{Var}[\xi_{j',l}']}$ where $\xi_{j,l}'=\alpha_{\text{RD},j,l}^2$. The coefficients $\rho_{j,j'}$ and $\rho_{j,j'}'$ represent the spatial correlation between two neighboring receive antennas and that between two neighboring transmit antennas, respectively, both at the relay. For analytical simplicity, we assume that $\rho_{j,j'}=\rho_{j,j'}'=\varrho^{|j-j'|}$, where $0\leq\rho\leq 1$ and $j,j'=1,2,\ldots,M$. Typically, equispaced linear antenna arrays are of this form of spatial correlation. Under this assumption and for the case of $L=1$, the CDF of $\mathcal{E}_u$ is given by [59, eq. (15)]

$$\begin{aligned}F_{\mathcal{E}_u}(x)=\frac{(1-\rho)^{m_{\text{SR}}}}{(m_{\text{SR}}-1)!}\sum_{i_1=0}^{\infty}\sum_{i_2=0}^{\infty}\cdots\sum_{i_{M-1}=0}^{\infty}\left[\prod_{v=1}^{M-1}\frac{\rho^{i_v}}{i_v!\,(m_{\text{SR}}+i_v-1)!}\right]\\ \times\Bigg\{\gamma\left(m_{\text{SR}}+i_1,\frac{x}{\Phi_{\text{SR},0}(1-\rho)}\right)\gamma\left(m_{\text{SR}}+i_{M-1},\frac{x}{\Phi_{\text{SR},0}(1-\rho)}\right)\\ \times\prod_{c=2}^{M-1}\gamma\left(m_{\text{SR}}+i_c+i_{c-1},\frac{(1+\rho)\,x}{\Phi_{\text{SR},0}(1-\rho)}\right)\Big/(1+\rho)^{m_{\text{SR}}+i_c+i_{c-1}}\Bigg\}U(x).\end{aligned} \tag{74}$$

From (74), we can obtain the PDF of $\mathcal{E}_u$ as (75), shown at the top of the next page. Likewise, the CDF and PDF of $\mathcal{E}_w'$ are obtained as (74) and (75), respectively, both with m_{SR} being replaced by m_{RD} and $\Phi_{\text{SR},0}$ being replaced by $\Phi_{\text{RD},0}$. To the best of our knowledge, however, there are no closed-form expressions for the CDFs and PDFs of $\mathcal{E}_u$ and $\mathcal{E}_w'$ in the case of $L>1$.

B. Derivation of $\mathcal{J}_2$

Using (72) and (73), the integral $\mathcal{J}_2$ in (14) can be rewritten as

$$\mathcal{J}_2=\mathcal{J}_3+\mathcal{J}_4+\mathcal{J}_5+\mathcal{J}_6 \tag{76}$$

where the expressions of $\{\mathcal{J}_n\}_{n=3}^{6}$ are given, respectively, in (77)-(80) on the page after the next page. The second equalities in (77) and (78) are obtained by using [30, eq. (3.381.3)], while the ones in (79) and (80) are obtained by changing the limits of integration and using [30, eq. (1.111)] and [30, eq. (3.471.9)]. Combining (76)-(80) gives (16).

$$
\begin{aligned}
f_{\mathcal{E}_u}(x) = {} & \frac{x^{m_{\mathrm{SR}}-1}}{\Phi_{\mathrm{SR},0}^{m_{\mathrm{SR}}}(m_{\mathrm{SR}}-1)!}\exp\!\left(-\frac{x}{\Phi_{\mathrm{SR},0}(1-\rho)}\right)\sum_{i_1=0}^{\infty}\sum_{i_2=0}^{\infty}\cdots\sum_{i_{M-1}=0}^{\infty}\left[\prod_{v=1}^{M-1}\frac{\rho^{i_v}}{i_v!\,(m_{\mathrm{SR}}+i_v-1)!}\right] \\
& \times\left\{\left[\left(\frac{x}{\Phi_{\mathrm{SR},0}(1-\rho)}\right)^{i_1}\Upsilon\left(m_{\mathrm{SR}}+i_{M-1},\frac{x}{\Phi_{\mathrm{SR},0}(1-\rho)}\right)+\left(\frac{x}{\Phi_{\mathrm{SR},0}(1-\rho)}\right)^{i_{M-1}}\Upsilon\left(m_{\mathrm{SR}}+i_1,\frac{x}{\Phi_{\mathrm{SR},0}(1-\rho)}\right)\right]\right. \\
& \times\prod_{c=2}^{M-1}\Upsilon\left(m_{\mathrm{SR}}+i_c+i_{c-1},\frac{(1+\rho)\,x}{\Phi_{\mathrm{SR},0}(1-\rho)}\right)\Big/(1+\rho)^{m_{\mathrm{SR}}+i_c+i_{c-1}} \\
& +\exp\!\left(-\frac{\rho\,x}{\Phi_{\mathrm{SR},0}(1-\rho)}\right)\Upsilon\left(m_{\mathrm{SR}}+i_1,\frac{x}{\Phi_{\mathrm{SR},0}(1-\rho)}\right)\Upsilon\left(m_{\mathrm{SR}}+i_{M-1},\frac{x}{\Phi_{\mathrm{SR},0}(1-\rho)}\right) \\
& \left.\times\sum_{p=2}^{M-1}\left(\frac{x}{\Phi_{\mathrm{SR},0}(1-\rho)}\right)^{i_p+i_{p-1}}\prod_{c=2,c\neq p}^{M-1}\Upsilon\left(m_{\mathrm{SR}}+i_c+i_{c-1},\frac{(1+\rho)\,x}{\Phi_{\mathrm{SR},0}(1-\rho)}\right)\Big/(1+\rho)^{m_{\mathrm{SR}}+i_c+i_{c-1}}\right\}U(x).
\end{aligned}
\tag{75}
$$

REFERENCES

[1] M. Z. Win and R. A. Scholtz, "Impulse radio: How it works," *IEEE Commun. Lett.*, vol. 2, no. 2, pp. 36–38, Feb. 1998.

[2] S. Roy, J. R. Foerster, V. S. Somayazulu, and D. G. Leeper, "Ultrawideband radio design: The promise of high-speed, short-range wireless connectivity," *Proc. IEEE*, vol. 92, no. 2, pp. 295–311, Feb. 2004.

[3] Federal Communications Commission (FCC), "First report and order in the matter of revision of part 15 of the commission's rules regarding ultra-wideband transmission systems," *Tech. Rep. ET Docket 98-153, FCC 02-48*, Apr. 2002.

[4] R. Pabst, B. H. Walke, D. C. Schultz, P. Herhold, H. Yanikomeroglu, S. Mukherjee, H. Viswanathan, M. Lott, W. Zirwas, M. Dohler, H. Aghvami, D. D. Falconer, and G. P. Fettweis, "Relay-based deployment concepts for wireless and mobile broadband radio," *IEEE Commun. Mag.*, vol. 42, no. 9, pp. 80–89, Sep. 2004.

[5] C. Cho, H. Zhang, and M. Nakagawa, "A UWB repeater with a short relaying-delay for range extension," in *Proc. IEEE WCNC*, vol. 2, Atlanta, GA, Mar. 2004, pp. 1154–1158.

[6] T. Q. S. Quek, M. Z. Win, and M. Chiani, "Distributed diversity in ultrawide bandwidth wireless sensor networks," in *Proc. IEEE VTC*, vol. 2, Stockholm, Sweden, May 2005, pp. 1355–1359.

[7] C. Abou-Rjeily, N. Daniele, and J.-C. Belfiore, "On the decode-and-forward cooperative diversity with coherent and non-coherent UWB systems," in *Proc. IEEE ICUWB*, Waltham, MA, Sep. 2006, pp. 435–440.

[8] C. Cho, H. Zhang, and M. Nakagawa, "A short delay relay scheme using shared frequency repeater for UWB impulse radio," *IEICE Trans. Fundam. Electron. Commun. Comput. Sci.*, vol. E90-A, no. 7, pp. 1444–1451, Jul. 2007.

[9] S. Zhu and K. K. Leung, "Cooperative orthogonal MIMO-relaying for UWB ad-hoc networks," in *Proc. IEEE GLOBECOM*, Washington, DC, Nov. 2007, pp. 5175–5179.

[10] C. Abou-Rjeily, N. Daniele, and J.-C. Belfiore, "On the amplify-and-forward cooperative diversity with time-hopping ultra-wideband communications," *IEEE Trans. Commun.*, vol. 56, no. 4, pp. 630–641, Apr. 2008.

[11] K. Maichalernnukul, T. Kaiser, and F. Zheng, "Rake fingers versus multiple antennas for UWB relay systems – Which one is better?" in *Proc. IEEE ICUWB*, vol. 1, Hannover, Germany, Sep. 2008, pp. 63–66.

[12] ——, "Performance investigation of a UWB relay system using multiple relays with multiple antennas in IEEE 802.15.3a channel," in *Proc. IEEE VTC*, Barcelona, Spain, Apr. 2009, pp. 1–6.

[13] A. Adinoyi and H. Yanikomeroglu, "Cooperative relaying in multi-antenna fixed relay networks," *IEEE Trans. Wireless Commun.*, vol. 6, no. 2, pp. 533–544, Feb. 2007.

[14] A. F. Molisch and M. Z. Win, "MIMO systems with antenna selection," *IEEE Microwave Mag.*, vol. 5, no. 1, pp. 46–56, Mar. 2004.

[15] S. Sanayei and A. Nosratinia, "Antenna selection in MIMO systems," *IEEE Commun. Mag.*, vol. 42, no. 10, pp. 68–73, Oct. 2004.

[16] J.-B. Kim and D. Kim, "End-to-end BER performance of cooperative MIMO transmission with antenna selection in Rayleigh fading," in *Proc. ACSSC*, Pacific Grove, CA, Oct. 2006, pp. 1654–1657.

[17] J. D. Choi and W. E. Stark, "Performance of ultra-wideband communications with suboptimal receiver in multipath channels," *IEEE J. Sel. Areas Commun.*, vol. 20, no. 9, pp. 1754–1766, Dec. 2002.

[18] A. Bletsas, H. Shin, and M. Z. Win, "Cooperative communications with outage-optimal opportunistic relaying," *IEEE Trans. Wireless Commun.*, vol. 6, no. 9, pp. 3450–3460, Sep. 2007.

[19] E. Beres and R. Adve, "Selection cooperation in multi-source cooperative networks," *IEEE Trans. Wireless Commun.*, vol. 7, no. 1, pp. 118–127, Jan. 2008.

[20] A. Adinoyi, Y. Fan, H. Yanikomeroglu, and H. V. Poor, "On the performance of selection relaying," in *Proc. IEEE VTC*, Calgary, Canada, Sep. 2008, pp. 1–5.

[21] B. Radunović and J.-Y. Le Boudec, "Optimal power control, scheduling, and routing in UWB networks," *IEEE J. Sel. Areas Commun.*, vol. 22, no. 7, pp. 1252–1270, Sep. 2004.

[22] S. Zhu and K. K. Leung, "Distributed cooperative routing for UWB ad-hoc networks," in *Proc. IEEE ICC*, Glasgow, Scotland, Jun. 2007, pp. 3339–3344.

[23] W. P. Siriwongpairat, A. K. Sadek, and K. J. R. Liu, "Bandwidth-efficient OFDM cooperative protocol with applications to UWB communications," in *Proc. IEEE WCNC*, New Orleans, GA, Apr. 2006, pp. 1729–1734.

[24] W. Q. Malik, "Spatial correlation in ultrawideband channels," *IEEE Trans. Wireless Commun.*, vol. 7, no. 2, pp. 604–610, Feb. 2008.

[25] J. N. Laneman, D. N. C. Tse, and G. W. Wornell, "Cooperative diversity in wireless networks: Efficient protocols and outage behavior," *IEEE Trans. on Inform. Theory*, vol. 50, no. 12, pp. 3062–3080, Dec. 2004.

[26] P. Larsson, N. Johansson, and K.-E. Sunell, "Coded bi-directional relaying," in *Proc. IEEE VTC*, vol. 2, Melbourne, Australia, May 2006, pp. 851–855.

$$\begin{aligned}\mathcal{J}_3 &= M\sum_{l=0}^{L-1}\sum_{k=1}^{m_{\mathrm{SR}}}\frac{\Delta(l,k,m_{\mathrm{SR}},\{\Phi_{\mathrm{SR},\ell}\}_{\ell=0}^{L-1})}{\Phi_{\mathrm{SR},l}^{k}(k-1)!}\int_{\frac{\gamma_{\mathrm{th}}}{\varrho_{\mathrm{S}}}}^{\infty}x^{k-1}\exp\!\left(-\frac{x}{\Phi_{\mathrm{SR},l}}\right)dx\\ &= M\sum_{l=0}^{L-1}\sum_{k=1}^{m_{\mathrm{SR}}}\Delta(l,k,m_{\mathrm{SR}},\{\Phi_{\mathrm{SR},\ell}\}_{\ell=0}^{L-1})\exp\!\left(-\frac{\gamma_{\mathrm{th}}}{\Phi_{\mathrm{SR},l}\,\varrho_{\mathrm{S}}}\right)\sum_{c=0}^{k-1}\frac{\left(\frac{\gamma_{\mathrm{th}}}{\Phi_{\mathrm{SR},l}\,\varrho_{\mathrm{S}}}\right)^{c}}{c\,!},\end{aligned} \tag{77}$$

$$\begin{aligned}\mathcal{J}_4 &= M\sum_{l=0}^{L-1}\sum_{k=1}^{m_{\mathrm{SR}}}\frac{\Delta(l,k,m_{\mathrm{SR}},\{\Phi_{\mathrm{SR},\ell}\}_{\ell=0}^{L-1})}{\Phi_{\mathrm{SR},l}^{k}(k-1)!}\sum_{v=1}^{M-1}(-1)^{v}\binom{M-1}{v}\sum_{l_1=0}^{L-1}\sum_{k_1=1}^{m_{\mathrm{SR}}}\cdots\sum_{l_v=0}^{L-1}\sum_{k_v=1}^{m_{\mathrm{SR}}}\prod_{p=1}^{v}\Xi_{k_p}\\ &\quad\times\int_{\frac{\gamma_{\mathrm{th}}}{\varrho_{\mathrm{S}}}}^{\infty}x^{A_1+k-1}\exp\!\left(-\left(A_2+\frac{1}{\Phi_{\mathrm{SR},l}}\right)x\right)dx\\ &= M\sum_{l=0}^{L-1}\sum_{k=1}^{m_{\mathrm{SR}}}\frac{\Delta(l,k,m_{\mathrm{SR}},\{\Phi_{\mathrm{SR},\ell}\}_{\ell=0}^{L-1})}{\Phi_{\mathrm{SR},l}^{k}(k-1)!}\sum_{v=1}^{M-1}(-1)^{v}\binom{M-1}{v}\sum_{l_1=0}^{L-1}\sum_{k_1=1}^{m_{\mathrm{SR}}}\cdots\sum_{l_v=0}^{L-1}\sum_{k_v=1}^{m_{\mathrm{SR}}}\prod_{p=1}^{v}\Xi_{k_p}\\ &\quad\times\quad\left(A_1+k,\frac{\gamma_{\mathrm{th}}}{\varrho_{\mathrm{S}}}\left(A_2+\frac{1}{\Phi_{\mathrm{SR},l}}\right)\right)\left(A_2+\frac{1}{\Phi_{\mathrm{SR},l}}\right)^{-A_1-k},\end{aligned} \tag{78}$$

$$\begin{aligned}\mathcal{J}_5 &= M\sum_{l=0}^{L-1}\sum_{k=1}^{m_{\mathrm{SR}}}\frac{\Delta(l,k,m_{\mathrm{SR}},\{\Phi_{\mathrm{SR},\ell}\}_{\ell=0}^{L-1})}{\Phi_{\mathrm{SR},l}^{k}(k-1)!}\sum_{v'=1}^{M}(-1)^{v'}\binom{M}{v'}\sum_{l'_1=0}^{L-1}\sum_{k'_1=1}^{m_{\mathrm{RD}}}\cdots\sum_{l'_{v'}=0}^{L-1}\sum_{k'_{v'}=1}^{m_{\mathrm{RD}}}\prod_{p'=1}^{v'}\Xi'_{k'_{p'}}\\ &\quad\times\int_{\frac{\gamma_{\mathrm{th}}}{\varrho_{\mathrm{S}}}}^{\infty}x^{k-1}\left(\frac{\gamma_{\mathrm{th}}(\varrho_{\mathrm{S}}\,x+1)}{\varrho_{\mathrm{S}}\,\varrho_{\mathrm{R}}\,x-\varrho_{\mathrm{R}}\gamma_{\mathrm{th}}}\right)^{A_3}\exp\!\left(-\frac{x}{\Phi_{\mathrm{SR},l}}-\frac{A_4\gamma_{\mathrm{th}}(\varrho_{\mathrm{S}}\,x+1)}{\varrho_{\mathrm{S}}\,\varrho_{\mathrm{R}}\,x-\varrho_{\mathrm{R}}\gamma_{\mathrm{th}}}\right)dx\\ &= 2M\sum_{l=0}^{L-1}\sum_{k=1}^{m_{\mathrm{SR}}}\frac{\Delta(l,k,m_{\mathrm{SR}},\{\Phi_{\mathrm{SR},\ell}\}_{\ell=0}^{L-1})}{\Phi_{\mathrm{SR},l}^{k}(k-1)!}\sum_{v'=1}^{M}(-1)^{v'}\binom{M}{v'}\sum_{l'_1=0}^{L-1}\sum_{k'_1=1}^{m_{\mathrm{RD}}}\cdots\sum_{l'_{v'}=0}^{L-1}\sum_{k'_{v'}=1}^{m_{\mathrm{RD}}}\prod_{p'=1}^{v'}\Xi'_{k'_{p'}}\\ &\quad\times\left(\frac{\gamma_{\mathrm{th}}}{\varrho_{\mathrm{S}}}\right)^{k}\left(\frac{\gamma_{\mathrm{th}}}{\varrho_{\mathrm{R}}}\right)^{A_3}\sqrt{A_4\Phi_{\mathrm{SR},l}\frac{\varrho_{\mathrm{S}}}{\varrho_{\mathrm{R}}}\left(1+\frac{1}{\gamma_{\mathrm{th}}}\right)}\exp\!\left(-\frac{A_4\gamma_{\mathrm{th}}}{\varrho_{\mathrm{R}}}-\frac{\gamma_{\mathrm{th}}}{\Phi_{\mathrm{SR},l}\,\varrho_{\mathrm{S}}}\right)\sum_{j_1=0}^{A_3}\binom{A_3}{j_1}\left[\frac{\varrho_{\mathrm{R}}}{A_4\Phi_{\mathrm{SR},l}\,\varrho_{\mathrm{S}}}\left(1+\frac{1}{\gamma_{\mathrm{th}}}\right)\right]^{\frac{j_1}{2}}\\ &\quad\times\sum_{j_2=0}^{k-1}\binom{k-1}{j_2}\left[A_4\Phi_{\mathrm{SR},l}\frac{\varrho_{\mathrm{S}}}{\varrho_{\mathrm{R}}}\left(1+\frac{1}{\gamma_{\mathrm{th}}}\right)\right]^{\frac{j_2}{2}}\mathcal{K}_{j_2-j_1+1}\left(2\sqrt{\frac{A_4\gamma_{\mathrm{th}}(\gamma_{\mathrm{th}}+1)}{\Phi_{\mathrm{SR},l}\,\varrho_{\mathrm{S}}\,\varrho_{\mathrm{R}}}}\right),\end{aligned} \tag{79}$$

and

$$\begin{aligned}\mathcal{J}_6 &= M\sum_{l=0}^{L-1}\sum_{k=1}^{m_{\mathrm{SR}}}\frac{\Delta(l,k,m_{\mathrm{SR}},\{\Phi_{\mathrm{SR},\ell}\}_{\ell=0}^{L-1})}{\Phi_{\mathrm{SR},l}^{k}(k-1)!}\sum_{v=1}^{M-1}\sum_{v'=1}^{M}(-1)^{v+v'}\binom{M-1}{v}\binom{M}{v'}\\ &\quad\times\sum_{l_1=0}^{L-1}\sum_{l'_1=0}^{L-1}\sum_{k_1=1}^{m_{\mathrm{SR}}}\sum_{k'_1=1}^{m_{\mathrm{RD}}}\cdots\sum_{l_v=0}^{L-1}\sum_{l'_{v'}=0}^{L-1}\sum_{k_v=1}^{m_{\mathrm{SR}}}\sum_{k'_{v'}=1}^{m_{\mathrm{RD}}}\prod_{p=1}^{v}\prod_{p'=1}^{v'}\Xi_{k_p}\,\Xi'_{k'_{p'}}\\ &\quad\times\int_{\frac{\gamma_{\mathrm{th}}}{\varrho_{\mathrm{S}}}}^{\infty}x^{A_1+k-1}\left(\frac{\gamma_{\mathrm{th}}(\varrho_{\mathrm{S}}\,x+1)}{\varrho_{\mathrm{S}}\,\varrho_{\mathrm{R}}\,x-\varrho_{\mathrm{R}}\gamma_{\mathrm{th}}}\right)^{A_3}\exp\!\left(-\left(A_2+\frac{1}{\Phi_{\mathrm{SR},l}}\right)x-\frac{A_4\gamma_{\mathrm{th}}(\varrho_{\mathrm{S}}\,x+1)}{\varrho_{\mathrm{S}}\,\varrho_{\mathrm{R}}\,x-\varrho_{\mathrm{R}}\gamma_{\mathrm{th}}}\right)dx\\ &= 2M\sum_{l=0}^{L-1}\sum_{k=1}^{m_{\mathrm{SR}}}\frac{\Delta(l,k,m_{\mathrm{SR}},\{\Phi_{\mathrm{SR},\ell}\}_{\ell=0}^{L-1})}{\Phi_{\mathrm{SR},l}^{k}(k-1)!}\sum_{v=1}^{M-1}\sum_{v'=1}^{M}(-1)^{v+v'}\binom{M-1}{v}\binom{M}{v'}\\ &\quad\times\sum_{l_1=0}^{L-1}\sum_{l'_1=0}^{L-1}\sum_{k_1=1}^{m_{\mathrm{SR}}}\sum_{k'_1=1}^{m_{\mathrm{RD}}}\cdots\sum_{l_v=0}^{L-1}\sum_{l'_{v'}=0}^{L-1}\sum_{k_v=1}^{m_{\mathrm{SR}}}\sum_{k'_{v'}=1}^{m_{\mathrm{RD}}}\prod_{p=1}^{v}\prod_{p'=1}^{v'}\Xi_{k_p}\,\Xi'_{k'_{p'}}\left(\frac{\gamma_{\mathrm{th}}}{\varrho_{\mathrm{S}}}\right)^{A_1+k}\left(\frac{\gamma_{\mathrm{th}}}{\varrho_{\mathrm{R}}}\right)^{A_3}\sqrt{\frac{A_4\varrho_{\mathrm{S}}}{\varrho_{\mathrm{R}}}\left(\frac{1+1/\gamma_{\mathrm{th}}}{A_2+1/\Phi_{\mathrm{SR},l}}\right)}\\ &\quad\times\exp\!\left(-\frac{A_4\gamma_{\mathrm{th}}}{\varrho_{\mathrm{R}}}-\frac{\gamma_{\mathrm{th}}}{\varrho_{\mathrm{S}}}\left(A_2+\frac{1}{\Phi_{\mathrm{SR},l}}\right)\right)\sum_{j_3=0}^{A_3}\binom{A_3}{j_3}\left[\frac{\varrho_{\mathrm{R}}}{A_4\varrho_{\mathrm{S}}}\left(A_2+\frac{1}{\Phi_{\mathrm{SR},l}}\right)\left(1+\frac{1}{\gamma_{\mathrm{th}}}\right)\right]^{\frac{j_3}{2}}\\ &\quad\times\sum_{j_4=0}^{A_1+k-1}\binom{A_1+k-1}{j_4}\left[\frac{A_4\varrho_{\mathrm{S}}}{\varrho_{\mathrm{R}}}\left(\frac{1+1/\gamma_{\mathrm{th}}}{A_2+1/\Phi_{\mathrm{SR},l}}\right)\right]^{\frac{j_4}{2}}\mathcal{K}_{j_4-j_3+1}\left(2\sqrt{\left(A_2+\frac{1}{\Phi_{\mathrm{SR},l}}\right)\frac{A_4\gamma_{\mathrm{th}}(\gamma_{\mathrm{th}}+1)}{\varrho_{\mathrm{S}}\,\varrho_{\mathrm{R}}}}\right).\end{aligned} \tag{80}$$

[27] P. Popovski and H. Yumo, "Wireless network coding by amplify-and-forward for bi-directional traffic flows," *IEEE Commun, Lett.*, vol. 11, no. 1, pp. 16–18, Jan. 2007.

[28] B. Rankov and A. Wittneben, "Spectral efficient protocols for half-duplex fading relay channels," *IEEE J. Sel. Areas Commun.*, vol. 25, no. 2, pp. 379–389, Feb. 2007.

[29] T. J. Oechtering and H. Boche, "Bidirectional regenerative half-duplex relaying using relay selection," *IEEE Trans. Wireless Commun.*, vol. 7, no. 5, pp. 1879–1888, May 2008.

[30] S. Gradshteyn and I. M. Ryzhik, *Table of Integrals, Series, and Products*, 6th ed. NY: Academic Press, 2000.

[31] D. Cassioli, M. Z. Win, and A. F. Molisch, "The ultra-wide bandwidth indoor channel: From statistical model to simulations," *IEEE J. Sel. Areas Commun.*, vol. 20, no. 6, pp. 1247–1257, Aug. 2002.

[32] J. Karedal, S. Wyne, P. Almers, F. Tufvesson, and A. F. Molisch, "Statistical analysis of the UWB channel in an industrial environment," in *Proc. IEEE VTC*, Los Angeles, CA, Sep. 2004, pp. 81–85.

[33] A. F. Molisch, J. R. Foerster, and M. Pendergrass, "Channel models for ultrawideband personal area networks," *IEEE Pers. Commun. Mag.*, vol. 10, no. 6, pp. 14–21, Dec. 2003.

[34] A. F. Molisch, D. Cassioli, C.-C. Chong, S. Emami, A. Fort, B. Kannan, J. Karedal, J. Kunisch, H. G. Schantz, K. Siwiak, and M. Z. Win, "A comprehensive standardized model for ultrawideband propagation channels," *IEEE Trans. Antennas Propag.*, vol. 54, no. 11, pp. 3151–3166, Nov. 2006.

[35] J. R. Foerster, "Channel modeling sub-committee report final," Tech. Rep. IEEE P802.15-02/490r1-SG3a, Feb. 2003.

[36] A. F. Molisch, K. Balakrishnan, D. Cassioli, C.-C. Chong, S. Emami, A. Fort, J. Karedal, J. Kunisch, H. G. Schantz, U. Schuster, and K. Siwiak, "IEEE 802.15.4a channel model – final report," Tech. Rep. IEEE 802.15-04-0662-02-004a, Nov. 2004.

[37] M.-G. Di Benedetto and G. Giancola, *Understanding Ultra Wide Band Radio Fundamentals*. NJ: Prentice-Hall PTR, 2004, ch. 8.

[38] H. Liu, R. C. Qiu, and Z. Tian, "Error performance of pulse-based ultra-wideband MIMO systems over indoor wireless channels," *IEEE Trans. Wireless Commun.*, vol. 4, no. 6, pp. 2939–2944, Nov. 2005.

[39] T. Kaiser, F. Zheng, and E. Dimitrov, "An overview of ultra-wide-band systems with MIMO," *Proc. IEEE*, vol. 97, no. 2, pp. 285–312, Feb. 2009.

[40] A. F. Molisch, "Ultrawideband propagation channels – Theory, measurement, and modeling," *IEEE Trans. Veh. Technol.*, vol. 54, no. 5, pp. 1528–1545, Sep. 2005.

[41] F. Zheng and T. Kaiser, "On the evaluation of channel capacity of UWB indoor wireless systems," *IEEE Trans. Signal Process.*, vol. 56, no. 12, pp. 6106–6113, Dec. 2008.

[42] D. Cassioli, M. Z. Win, F. Vatalaro, and A. F. Molisch, "Low complexity Rake receivers in ultra-wideband channels," *IEEE Trans. Wireless Commun.*, vol. 6, no. 4, pp. 1265–1275, Apr. 2007.

[43] T. Wang, A. Cano, G. B. Giannakis, and J. N. Laneman, "High-performance cooperative demodulation with decode-and-forward relays," *IEEE Trans. Commun.*, vol. 55, no. 7, pp. 1427–1438, Jul. 2007.

[44] L. Yang and G. B. Giannakis, "Analog space-time coding for multiantenna ultra-wideband transmissions," *IEEE Trans. Commun.*, vol. 52, no. 3, pp. 507–517, Mar. 2004.

[45] H. Chen, A. B. Gershman, and S. Shahbazpanahi, "Filter-and-forward distributed beamforming for relay networks in frequency selective fading channels," *IEEE Trans. Signal Process.*, vol. 58, no. 3, pp. 1251–1262, Mar. 2010.

[46] K. Usuda, H. Zhang, and M. Nakagawa, "Pre-Rake performance for pulse based UWB system in a standardized UWB short-range channel," in *Proc. IEEE WCNC*, vol. 2, Atlanta, GA, Mar. 2004, pp. 920–925.

[47] S. Imada and T. Ohtsuki, "Pre-Rake diversity combining for UWB systems in IEEE 802.15 UWB multipath channel," in *Proc. Joint UWBST & IWUWBS*, Kyoto, Japan, May 2004, pp. 236–240.

[48] M. Abramowitz and I. A. Stegun, *Handbook of Mathematical Functions with Formulas, Graphs, and Mathematical Tables*. NY: Dover Press, 1970.

[49] A. Bletsas, A. Khisti, D. P. Reed, and A. Lippman, "A simple cooperative diversity method based on network path selection," *IEEE J. Sel. Areas Commun.*, vol. 23, no. 4, pp. 659–672, Mar. 2006.

[50] K. Maichalernnukul, T. Kaiser, and F. Zheng, "Performance of dual-hop MIMO ultra-wideband transmissions: Preliminary results," in *Proc. CISS*, Baltimore, MD, Mar. 2009, pp. 118–123.

[51] R. C. Qiu, C. Zhou, N. Guo, and J. Q. Zhang, "Time reversal with MISO for ultrawideband communications: Experimental results," *IEEE Antennas Wireless Propag. Lett.*, vol. 5, no. 1, pp. 269–273, Dec. 2006.

[52] K.-S. Hwang, Y.-C. Ko, and M.-S. Alouini, "Two-way amplify and forward relaying with adaptive modulation," in *Proc. IWCMC*, Leipzig, Germany, Jun. 2009, pp. 1370–1374.

[53] Y. Ishiyama and T. Ohtsuki, "Performance comparison of UWB-IR using Rake receivers in UWB channel models," in *Proc. Joint UWBST & IWUWBS*, Kyoto, Japan, May 2004, pp. 226–230.

[54] O. H. Bustos, A. G. Flesia, and A. C. Frery, "Generalized method for sampling spatially correlated heterogeneous speckled imagery," *EURASIP J. Applied Signal Process.*, vol. 2, pp. 89–99, 2001.

[55] S. S. Ghassemzadeh and V. Tarokh, "UWB path loss characterization in residential environments," in *Proc. IEEE MTT-S IMS*, vol. 1, Jun. 2003, pp. 365–368.

[56] E. Al-Hussaini and A. Al-Bassiouni, "Performance of MRC diversity systems for the detection of signals with Nakagami fading," *IEEE Trans. Commun.*, vol. 33, no. 12, pp. 1315–1319, Dec. 1985.

[57] G. K. Karagiannidis, N. C. Sagias, and T. A. Tsiftsis, "Closed-form statistics for the sum of squared Nakagami-*m* variates and its applications," *IEEE Trans. Commun.*, vol. 54, no. 8, pp. 1353–1359, Aug. 2006.

[58] A. Papoulis, *Probability, Random Variables, and Stochastic Processes*. NY: McGraw-Hill, 1991.

[59] V. A. Aalo and T. Piboongungon, "On the multivariate generalized Gamma distribution with exponential correlation," in *Proc. IEEE GLOBECOM*, St. Louis, MO, Nov. 2005, pp. 1229–1233.

Kiattisak Maichalernnukul received the B.E. and M.E. degrees from Chulalongkorn University, Thailand, in 2002 and 2004, respectively, and the Dr.-Ing. degree from University of Hannover, Germany, in 2010, all in electrical engineering.

From 2005 to 2006, he was a Research Assistant with the National Electronics and Computer Technology Center, Thailand. From 2007 to 2011, he was a Scientific Assistant with the Institute of Communications Technology, University of Hannover. Since July 2011, he has been a Lecturer with Rangsit University, Thailand. His research interests are in the areas of communication theory and signal processing for wireless communications.